Atmos. Meas. Tech. Discuss., 6, 2253–2325, 2013
www.atmos-meas-tech-discuss.net/6/2253/2013/
doi:10.5194/amtd-6-2253-2013

Atmospheric Measurement Techniques Discussions

Enhancement of aerosol characterization using synergy of lidar and sun – photometer coincident observations: the GARRLiC algorithm

A. Lopatin[1,2], O. Dubovik[2], A. Chaikovsky[1], Ph. Goloub[2], T. Lapyonok[2], D. Tanré[2], and P. Litvinov[2]

[1]Laboratory of scattering media, NASB – B.I. Stepanov Institute of Physics, Minsk, Belarus
[2]Laboratoire d'Optique Atmosphérique, UMR8518, CNRS – Université de Lille 1, Villeneuve d'Ascq, France

Received: 29 January 2013 – Accepted: 20 February 2013 – Published: 1 March 2013

Correspondence to: A. Lopatin (anton.lapatsin@ed.univ-lille1.fr, lopatsin@scat.bas-net.by)

Published by Copernicus Publications on behalf of the European Geosciences Union.

Abstract

Currently most of experiments pursuing comprehensive characterization of atmosphere include coordinated observations by both lidar and radiometers in order to obtain important complimentary information about aerosol properties. The passive observations by radiometers from ground are mostly sensitive to the properties of aerosol in total atmospheric column and have very limited sensitivity to vertical structure of the atmosphere. Such observations are commonly used for measuring aerosol optical thickness and deriving the information about aerosol microphysics including aerosol particles shape, size distribution, and complex refractive index. In a contrast, lidar observations of atmospheric responses from different altitudes to laser pulses emitted from ground are designed to provide accurate profiling of the atmospheric properties. The interpretation of the lidar observation generally relies on some assumptions about aerosol type and loading. Here we present the GARRLiC algorithm (Generalized Aerosol Retrieval from Radiometer and Lidar Combined data) that simultaneously inverts co-incident lidar and radiometer observations and derives a united set of aerosol parameters. Such synergetic retrieval is expected to result in additional enhancements in derived aerosol properties because the backscattering observations by lidar add some sensitivity to the columnar properties of aerosol, while radiometric observations provide sufficient constraints on aerosol type and loading that generally are missing in lidar signals.

GARRLiC is based on AERONET algorithm for inverting combined observations by radiometer and multi-wavelength elastic lidar observations. It is expected that spectral changes of backscattering signal obtained by multi-wavelength lidar at different altitudes provide some sensitivity to the vertical variability of aerosol particle sizes. In order to benefit from this sensitivity the algorithm is set to derive not only the vertical profile of total aerosol concentration but it also differentiates between the contributions of fine and coarse modes of aerosol. The detailed microphysical properties are assumed height independent and different for each mode and expected to be derived as

AMTD
6, 2253–2325, 2013

a part of the retrieval. Thus, the GARRLiC inversion algorithm retrieves vertical distribution of both fine and coarse aerosol concentrations as well as the size distribution, complex refractive index and single scattering albedo for each mode.

The potential and limitations of the method are demonstrated by the series of sensitivity tests. The practical outcome of the approach is illustrated by applications of the algorithm to the real lidar and radiometer observations obtained over selected AERONET site.

1 Introduction

Atmospheric aerosols are known to be important part of the complex physical-chemical processes that impact Earth climate. Such impacts take their effects both on global and regional scales (e.g. D'Almeida et al., 1991; Charlson et al., 1992; Hobbs, 1993; Pilinis et al., 1995; Ramanathan et al., 2001; Forster et al., 2007; Hansen et al., 2011). Being common atmosphere pollutant aerosols also have influence on population health (e.g. Jones, 1999; Harrison and Yin, 2000) and ecological equilibrium (e.g. Barker and Tingey, 1992).

In order to estimate these impacts large variety of methods for monitoring atmospheric aerosols were developed. Among others remote sensing methods, both active and passive, proved to be fruitful and convenient. A number of developed and launched space instruments (e.g. Bréon et al., 2002; Winker et al., 2007) provide global monitoring of aerosol properties (e.g. King et al., 1999; Kokhanovsky et al., 2007). Observations by ground-based instruments generally provide more detailed and accurate information about aerosol properties (e.g. Nakajima et al., 1996; Dubovik and King, 2000) but cover only local area nearby the observation site. In order to obtain such data at extended geographical scales, the ground-based observations are often collected within observational networks employing identical instrumentation and standardized data processing procedures. At present there is a number of global and regional networks conducting both passive and active ground-based observations. For example,

AMTD
6, 2253–2325, 2013

global AERONET (Holben, 1998) and South-Eastern SKYNET (Nakajima et al., 2007) networks of sun-photometers, as well as, a variety of lidar networks including regional EARLINET (Bösenberg, 2000), ADNET (Murayama et al., 2001), MPL-Net (Welton et al., 2002), ALiNe (Antuña et al., 2006), Cis-LiNet (Chaikovsky et al., 2006b) and a recent global lidar network GALION (Bösenberg and Hoff, 2007) have been established during two last decades. Aerosol data collected by these networks provide valuable aerosol information that is widely used for validating satellite observations (e.g. Remer et al., 2002, 2005; Schuster et al., 2012; Hasekamp et al., 2011; Yoon et al., 2011; Kahn et al., 2010; Ahmad et al., 2010) and constraining aerosol properties in climate simulation efforts (e.g. Kinne et al., 2003, 2006; Textor et al., 2006; Koch et al., 2009).

Despite of the achieved progress in aerosol remote sensing the limited accuracy in the knowledge of aerosol properties remains one of the main uncertainties in climate assessments (Forster et al., 2007; Hansen et al., 2011). The expected improvements in the ground-based aerosol monitoring are associated with two kinds of efforts: (i) enhancement of the observation completeness by employing a variety of complimentary observational techniques and (ii) improvement of the accuracy of derived aerosol information. For example, the number of extensive multi-instrumental aerosol campaigns have been organized (e.g. Ramanathan et al., 2001; Müller et al., 2003; McKendry et al., 2007; Papayannis et al., 2005; Holben et al., 2011). In addition, the number of permanent monitoring sites equipped with several instruments is continuously increasing (e.g. Takamura et al., 1994; Waquet et al., 2005; Müller et al., 2004; Ansmann et al., 2010). In these regards, the columnar properties of aerosol derived by the photometers and aerosol vertical profiles provided by the lidars are clearly complimentary pieces of information about aerosol both important for climatic studies. Specifically, the columnar properties are important for direct aerosol forcing estimations both on global and regional scale (Pilinis et al., 1995; Costa et al., 2004). On the other hand vertical structure of the aerosol is needed for accounting of the indirect effects like influence on cloud formation (McCormick et al., 1993; Bréon, 2006). The importance of obtaining simultaneous information about both columnar and vertical aerosol properties is rather

AMTD
6, 2253–2325, 2013

evident for scientific community, and, a substantial number of sites within ground-based networks conducting co-incident lidar and photometric measurements have been established.

In addition, the accumulation of a variety of complementary data is not the only positive effect. It also helps to improve the accuracy of the obtained data and derive qualitatively new aerosol characteristics. Indeed, processing of both passive and active remote measurements rely on a set of several assumptions. For example, retrievals of aerosol columnar properties from passive methods use an assumption of the vertical distribution of aerosol. The uncertainties in this assumption may have a notable effect on the retrieval result, especially in cases of polarimetric observations. Retrievals from active sounding, on the other hand, deal with relatively limited information from the altitude profiles of the spectral backscattering and usually rely on assumptions about aerosol columnar properties. For example, information about aerosol type is usually used for constraining the lidar ratio that defines relation between aerosol backscatter and extinction. Combined with known boundary conditions, this provides missing information and allows quantitative interpretation of lidar signals and retrieval of vertical profiles of aerosol backscatter and extinction (Klett, 1981, 1985). Commonly lidar ratio is chosen using a priori climatological data sets. For example, processing of lidar observations from CALIPSO space-borne platform relies on the lidar ratio climatological models derived by cluster analysis from entire database of AERONET retrievals (Omar et al., 2005). However, inconsistencies in the chosen lidar ratio directly propagate into derived results and may strongly affect the lidar retrievals (Sasano et al., 1985; Kovalev, 1995). The most reliable and therefore preferable approach is to define lidar ratio using co-incident measurement by developing enhanced lidar capabilities or by obtaining missing information from another instruments (Ferrare et al., 1998a; Gobbi et al., 2003). For example, enhancement of lidar observation can be achieved by employing lidar systems registering combined elastic-Raman signals (Ansmann et al., 1992; Ferrare et al., 1998a,b; Turner et al., 2002), using slope methods (Gutkowicz-Krusin, 1993; Sicard et al., 2002; Pahlow et al., 2004) or by conducting high spectral resolution

AMTD
6, 2253–2325, 2013

lidar observations (Shipley et al., 1983; Liu et al., 2002; Hair et al., 2008). Usage of approaches with non-elastic observations result in significant enhancement of the information contents in backscattering observations, which allows derivation of aerosol extinction profiles and even estimations of aerosol microphysical properties without a priori constraints on aerosol type or loading (Müller et al., 1999, 2005; Veselovskii et al., 2004). However, lidar systems with non-elastic capabilities are rather complex and often require special observational conditions (e.g. non-elastic signal is very weak during day time). Therefore, bulk of monitoring of vertical aerosol variability is conducted by conventional lidars and the constraining of aerosol type is done using co-incident airborne measurements by nephelometers (Hoff et al., 1996; Adam et al., 2004) or spectrophotometers (Marenco et al., 1997) or using ground-based measurements by sun-photometers (Waquet et al., 2005). The straightforward constraining of the lidar retrievals using values of total aerosol optical thickness (AOT) is a common way of utilizing co-incident sun-photometer measurements for improvement of lidar observations processing (Fernald et al., 1972; Fernald, 1984). In addition, several more sophisticated approaches of combining two types of measurements were proposed recently for exploring additional sensitivities in both lidar and photometric observations. Such methods are usually aimed not only at improving accuracy of the retrieved aerosol characteristics, but rather at retrieving qualitatively new aerosol information. For example, the most common lidar products include vertical profiles of extinction or/and concentration of aerosol that are derived using lidar ratio fixed under some assumptions about aerosol type. Co-incident data from sun-photometer provide the required information about aerosol type. However, aerosol type may change vertically, for example, when background aerosol is mixed with layers of transported aerosols as those from desert dust or biomass burning aerosols. Ground-based radiometric data have practically no sensitivity to vertical variability of aerosol; they can only provide some indication of possible aerosol mixtures. On the other hand, spectral (sensitive to variations of aerosol sizes) and polarimetric (sensitive to particle shape) lidar measurements can trace rather clear qualitative picture of aerosol vertical mixing. Utilization of such lidar

AMTD
6, 2253–2325, 2013

data in a combination with co-incident radiometric data allows some quantitative description of vertical distribution of aerosol mixtures.

Generally information about sizes and composition of aerosol particles obtained from radiometers is used for defining a number of different aerosol components and their detailed properties (size distributions, complex refractive index and particle shape). Then lidar data are fitted using optical properties of these assumed aerosol components by searching for their vertical mixing that provides the best match of lidar data. For example, studies by Chaikovsky et al. (2002, 2004, 2006a, 2012); Cuesta et al. (2008) used the measured spectral dependence of backscatter and extinction to derive vertical distribution of two optically distinct aerosol modes assuming that only concentrations of the each aerosol mode can change vertically. The size distributions and complex refractive indices of each aerosol component were fixed using the aerosol retrievals from AERONET radiometers. In the LiRIC (Lidar-Radiometer Inversion Code) algorithm (Chaikovsky et al., 2012) assumed two mono-modal fine and coarse aerosol components with size distributions obtained by dividing AERONET derived distribution into two using the minimum in the range of sizes from 0.194 µm to 0.576 µm as a separation point. The complex refractive index for both modes was assumed the same and equal to the one retrieved by AERONET. Cuesta et al. (2008) used more complex procedure. First, the AERONET size distribution was decomposed into log-normal mono-modal distributions. Then both bi-modal size distributions of each mode and complex refractive indices were defined using available ancillary data. Ansmann et al. (2011) used measured depolarization profiles in order to derive vertical distribution of spherical and non-spherical aerosol components with size distributions and complex refractive indices fixed from modelling.

The GARRLiC (Generalized Aerosol Retrieval from Radiometer and Lidar Combined data) approach proposed in this paper pursues even deeper synergy of lidar and radiometer data in the retrievals. Indeed, the methods described above are aimed at enhanced processing of lidar data and do not include any feedback on aerosol columnar properties. At the same time, some additional sensitivity to columnar properties

AMTD
6, 2253–2325, 2013

of aerosol compared to radiometric data is provided from lidar measurements. For example, the radiometric observations from ground do not include observation in back scattering direction. In addition, radiation field observed by the radiometers, in particular its polarimetric properties, has some sensitivity to aerosol vertical distribution but using this sensitivity is practically impossible without relying on independent information about vertical variability of aerosol. Therefore, the approach proposed here is aimed to take an advantage from all sensitivities in lidar and radiometric data to both vertical and columnar aerosol properties.

2 The GARRLiC algorithm concept

Both LiRIC and GARRLiC algorithms use positive heritage of the AERONET retrieval. For example, several key elements of statistically optimized inversion approach designed for AERONET by Dubovik and King (2000) were adapted in LiRIC. In addition, LiRIC uses the identical to AERONET model of aerosol microphysics. At the same time, LiRIC takes its roots from earlier lidar retrievals adopting some elements of the AERONET retrieval. In this regard, GARRLiC was created by direct modification of AERONET and PARASOL algorithms adapting them for inclusion of lidar data. The approach for treating lidar data strongly relies on LiRIC heritage. Therefore, below we will review the key aspects of all these algorithms that are used in the GARRLiC design.

The AERONET operational retrieval is implemented successfully for more than a decade by the algorithm described by Dubovik and King (2000). It had been tested (Dubovik et al., 2000), improved and upgraded over time. For example, the following new modelling aspects has been included: (i) accounting for particle non-sphericity in aerosol scattering (Dubovik et al., 2002b, 2006), (ii) simulation of bi-directional land and ocean surface properties (Sinyuk et al., 2007), (iii) both modelling of linear polarization and using the polarimetric measurements in the retrieval (Dubovik et al., 2006; Li et al., 2009). Years of the algorithm exploitation has shown possibility to provide new valuable details of aerosol properties (e.g. Dubovik et al., 2002a; Eck et al., 2005, 2012,

AMTD
6, 2253–2325, 2013

etc.). The algorithm by Dubovik and King (2000) has been developed with the idea to achieve high flexibility in using the various observations and deriving the extended set of aerosol parameters. Specifically, the algorithm is based (see Dubovik and King, 2000; Dubovik, 2004) on multi-term LSM (Least Square Method) that allows flexible and rigorous inversion of the various combinations of the independent multi-source measurements. As a result, the modifications of algorithm have been used for inverting the various combined data. For example, Sinyuk et al. (2007) used modified algorithm for deriving both aerosol and surface properties from co-incident observations of ground-based radiometer and satellite. Gatebe et al. (2010) have implemented a modification for inverting the combination of the ground-based AERONET observations with the airborne observations by the photometer and up- and down- looking radiometer and derived the detailed properties of aerosol both over and under airplane together with properties of surface reflectance. The latest modification of the algorithm has been developed by Dubovik et al. (2011) for retrieving both properties of aerosol and surface from observations of PARASOL/POLDER. This version of the algorithm generalizes and includes most of precedent modifications. Moreover, the main part of the computer routine realizing the algorithm has been significantly rewritten with the objective of the enhancing algorithm flexibility in order that it could be used in multiple applications with no or only minor modifications of the main body of the algorithm routine. The algorithm has nearly independent modules "forward model" and "numerical inversion" (see Fig. 1) in the respect that these modules can be modified independently. Correspondingly, if a possibility of simulating new measured atmospheric characteristic is included in the "forward model" this characteristic can be inverted with no modifications of the "numerical inversion" module in the source code. Only input parameters of the inversion program need to be changed. As a result, the algorithm by Dubovik et al. (2011) can be used with no modifications in multiple applications. For example, the same program can be used for aerosol retrieval from satellite (e.g. POLDER/PARASOL), ground-based (e.g. AERONET) or aircraft observations. In the present development we used this last version of the algorithm and modified it by adding a possibility to invert lidar

AMTD
6, 2253–2325, 2013

observations together with passive radiometric data. With that purpose modelling lidar observations was included in the "forward model" and "numerical inversion" module was adapted for inverting the combined radiometer and lidar observations. The details of these modifications are described in two following sections.

3 Modifications employed in the "forward model"

The previous versions of the retrieval code (Dubovik and King, 2000; Dubovik et al., 2011) and its modifications (Sinyuk et al., 2007; Gatebe et al., 2010) were developed for inverting only passive observations by ground-based, satellite and airborne radiometers. Therefore, for the needs of the current study a possibility of modelling lidar observations was included into the "forward model" module. The diagram in Fig. 2 illustrates the concept of accounting for the aerosol vertical variability in the "forward model" module of the present algorithm. Although the concept has significant similarities with LiRIC, it has several new aspects.

Similarly to the LiRIC, GARRLiC is designed to provide two independent vertical profiles of the concentrations of fine and coarse modes that are among the retrieved characteristics. Aerosol is described as a bi-component mixture of fine and coarse aerosol modes. The microphysical properties of each mode (particle sizes, complex index of refraction and shape) are height independent, while vertical profiles of concentrations vary with altitude. Such approach minimizes the amount of a priori estimations used in the retrieval, and it is expected to provide more detailed and accurate information about both vertical and columnar aerosol properties. In a contrast to LiRIC, in GARRLiC model the size intervals of the modes may overlap and the size independent complex refractive index may be different for each aerosol component.

AMTD
6, 2253–2325, 2013

3.1 Attenuated backscatter

The attenuated backscatter $L(\lambda, h)$ measured by lidar was modelled in single scattering approximation using lidar equation:

$$L(\lambda, h) = A(\lambda)\beta(\lambda, h)\exp\left(-2\int_0^h \sigma(\lambda, h')\,\mathrm{d}h'\right) \quad (1)$$

where $A(\lambda)$ is the lidar calibration parameter, $\sigma(\lambda, h)$ is the vertical profile of atmospheric extinction, and $\beta(\lambda, h)$ is the vertical profile of the atmospheric backscattering that is modelled using profiles of atmosphere single scattering albedo $\omega_0(\lambda, h)$ and the phase function $P_{11}(\Theta, \lambda, h)$ at scattering angle $\Theta = 180^\circ$ as follows:

$$\beta(\lambda, h) = \frac{1}{4\pi}\sigma(\lambda, h)\,\omega_0(\lambda, h)\,P_{11}(180^\circ, \lambda, h) \quad (2)$$

The extinction and backscattering of the atmosphere are affected by gaseous absorption, molecular scattering and aerosol scattering and absorption:

$$\sigma(\lambda, h) = \sigma_{\mathrm{gas}}^{\mathrm{abs}}(\lambda, h) + \sigma_{\mathrm{mol}}^{\mathrm{scat}}(\lambda, h) + \sigma_{\mathrm{aer}}^{\mathrm{ext}}(\lambda, h) \quad (3)$$

$$\beta(\lambda, h) = \beta_{\mathrm{mol}}(\lambda, h) + \beta_{\mathrm{aer}}(\lambda, h) \quad (4)$$

The lidar measurements are made in window channels (0.355, 0.532 and 1.064 µm) with very minor gaseous absorption that is accounted using known climatological data. The effects of molecular scattering are also can be accounted by usage of climatological data. Specifically, the phase function $P_{11}^{\mathrm{mol}}(180^\circ, \lambda, h)$ of molecular scattering is constant and well known. The variability of molecular scattering profile $\sigma_{\mathrm{mol}}^{\mathrm{scat}}(\lambda, h)$ over observation site can be simulated with acceptable accuracy based on the information about site geographical coordinates and elevation (Fleming et al. (1988),

AMTD
6, 2253–2325, 2013

http://ccmc.gsfc.nasa.gov/modelweb/atmos/cospar1.html). However, the aerosol properties $\sigma_{\text{aer}}^{\text{ext}}(\lambda, h)$ and $\beta_{\text{aer}}(\lambda, h)$ are highly variable and can not be modelled using climatologies. Therefore, in "forward model" these properties are driven by the parameters included in the vector of unknowns that are retrieved during inversion. The radiometric observations both from ground and space are mostly sensitive to columnar properties of aerosol, therefore the "forward model" in the previous version of the algorithm was driven by the parameters describing these columnar properties. The aerosol was assumed as a mixture of the several aerosol components. Each aerosol component was represented by a sum of spherical and non-spherical fractions. The spherical fraction was modelled as polydisperse mixture of the spheres. The non-spherical fraction was modelled as mixture of randomly oriented polydisperse spheroids. The distributions of particle volumes and the complex refractive indices were assumed the same in both spherical and non-spherical aerosol fractions. The extinction, absorption and scattering properties of the aerosol in the total atmospheric column were modelled as:

$$\tau_{\text{ext/abs}}(\lambda) = \sum_{k=1,\ldots,N_k} \left[\sum_{i=1,\ldots,N_i} \left(c_{\text{sph}} \mathbf{K}_{\text{ext/abs}}^{\text{sph}}(\ldots, r_i) + \left(1 - c_{\text{sph}}\right) \mathbf{K}_{\text{ext/abs}}^{\text{ns}}(\ldots, r_i) \right) \frac{\mathrm{d}V_k(r_i)}{\mathrm{d}\ln r} \right] \tag{5}$$

$$\omega_0(\lambda) P_{ij}(\Theta, \lambda) = \sum_{k=1,\ldots,N_k} \left[\sum_{i=1,\ldots,N_i} \left(c_{\text{sph}} \mathbf{K}_{ij}^{\text{sph}}(\ldots, r_i) + \left(1 - c_{\text{sph}}\right) \mathbf{K}_{ij}^{\text{ns}}(\ldots, r_i) \right) \frac{\mathrm{d}V_k(r_i)}{\mathrm{d}\ln r} \right] \tag{6}$$

where $\mathbf{K}_{\text{ext/abs}}^{\text{sph}}(\ldots, r_i)$ and $\mathbf{K}_{ij}^{\text{ns}}(\ldots, r_i)$ are the kernels of extinction, absorption and scattering properties of spherical and non-spherical aerosol fractions (Dubovik et al., 2011). For reducing calculation time in the numerical integration of spheroid optical properties over size and shape, these kernels were arranged as the look-up tables simulated for

AMTD
6, 2253–2325, 2013

quadrature coefficients employed as discussed in detail by Dubovik et al. (2006). The calculations of kernels for non-spherical fraction were done assuming non-spherical aerosol as a mixture of randomly oriented polydisperse spheroids with the distribution of the aspect ratios fixed to the one providing the best fit to the laboratory measurements of mineral dust (feldspar sample) phase matrices by Volten et al. (2001). Such strategy of accounting for non-spherical shape of desert dust aerosol is successfully used in the operational AERONET retrieval.

It is noteworthy that the spheroid model developed by Dubovik et al. (2002b, 2006) appeared to be rather useful for other aerosol remote sensing applications. It was shown that the spheroid model allows qualitative reproduction of the main features of lidar observations of non-spherical desert dust (Cattrall et al., 2005). Furthermore, Veselovskii et al. (2010) and Di Girolamo et al. (2012) have incorporated the spheroid model into the algorithm retrieving aerosol properties from lidar observations. That were, probably, one of the first attempts to interpret quantitatively the sensitivity of the lidar observations to particle non-sphericity.

It should be noted that Eqs. (5) and (6) are written for aerosol composed by $N_k\,(k = 1,..,N_k)$ components, where each component has different values of complex refractive index n_k, k_k and size distribution $\frac{dV_k(r_i)}{d\ln r}$. Such possibility of modelling multi-component aerosol is included in the previous version of the algorithm for both inverting ground based (Dubovik and King, 2000) and satellite (Dubovik et al., 2011) observations. In principle, such assumption allows for accurate modelling of scattering by mixes of aerosols of different types with distinctly different indices of the refraction. Such situations often appear in the reality, for example, when smoke is mixed with transported layer of desert dust. The differentiation and retrieval of both the size distributions and the complex refractive indices for each fraction of mixed aerosol from remote sensing is highly demanded and recommended (Mishchenko et al., 2007). However, due to the limited information content of radiometric observation, realizing such retrieval is a very challenging task. For example, sensitivity studies by Dubovik et al. (2000) demonstrated and studied such retrieval in a series of numerical tests with synthetic

AMTD
6, 2253–2325, 2013

AERONET data and found that the retrieval of bi-component ($N_k = 2$) aerosol was non-unique. Specifically, using different initial guesses the retrieval algorithm was finding several different bi-component aerosol mixtures providing equally good fit of the observations. As a result of this feature, the operational AERONET algorithm uses the assumption of mono-component aerosol with size independent complex refractive index. Nonetheless, in the present study we use bi-component aerosol model, where aerosol is composed by fine ($k = 1$) and coarse ($k = 2$) aerosol components with different size distributions and complex refractive indices. It is expected that combination of the observations by ground-based radiometer with the spectral lidar observations provide sufficient information for satisfactory retrieval of bi-component aerosol mixture properties. Indeed, the spectral observations of lidar have sensitivity to mixing of aerosol layers at different altitudes. This sensitivity should help to differentiate the properties of a bi-component mixture.

The vertical variability of atmosphere is modelled using vertical profiles of the volume concentrations $c_k(h)$ of the aerosol components under an assumption that such characteristics as: size distribution, complex refractive index and particle shape of each aerosol component are vertically independent. Therefore, aerosol backscattering $\beta_{\text{aer}}(\lambda, h)$ and extinction properties $\sigma_{\text{aer}}(\lambda, h)$ can be modelled as:

$$\beta_{\text{aer}}(\lambda, h) = \frac{1}{4\pi} \sum_{k=1,2} \sigma^k_{\text{aer}}(\lambda, h) \omega^k_0(\lambda) P^k_{11}(180°, \lambda) \tag{7}$$

and

$$\sigma^k_{\text{aer}}(\lambda, h) = \tau_k(\lambda) c_k(h) \tag{8}$$

where the vertical profiles of the volume concentrations $c_k(h)$ of aerosol components are normalized to unity: $\int_0^{h_{\text{TOA}}} c_k(h)\, \mathrm{d}h = 1$.

Thus, this approach is convenient for both modelling columnar aerosol properties by Eqs. (5) and (6) and vertical lidar observations by Eq. (1).

AMTD
6, 2253–2325, 2013

In addition, vertical variability of aerosol may have some effect on the outgoing atmospheric radiances measured from space (Dubovik et al., 2011). This variability is accounted by solving full radiative transfer equations in the plane parallel approximation using vertically dependent optical characteristics of the atmosphere:

$$\Delta\tau_i = \Delta\tau_i^{\text{gas}} + \Delta\tau_i^{\text{mol}} + \sum_{k=1,2} \Delta\tau_i^{\text{aer},k} \tag{9}$$

$$\omega_0(\lambda) = \frac{\Delta\tau_i{}^{\text{mol}} + \sum_{k=1,2} \Delta\tau_i^{\text{aer},k}\,\omega_0(\lambda)}{\Delta\tau_i^{\text{gas}} + \Delta\tau_i^{\text{mol}} + \sum_{k=1,2} \Delta\tau_i^{\text{aer},k}} \tag{10}$$

$$P_{ii}{}^{i}(\Theta,\lambda) = \frac{\Delta\tau_k{}^{\text{mol}} P_{ii}(\Theta,\lambda) + \sum_{k=1,2} \Delta\tau_i^{\text{aer},k}\,\omega_0^k(\lambda) P_{ii}{}^{\text{aer},k}(\Theta,\lambda)}{\Delta\tau_i{}^{\text{mol}} + \sum_{k=1,2} \Delta\tau_i^{\text{aer},k}\,\omega_0(\lambda)} \tag{11}$$

where $\Delta\tau_i$, $\omega_0^i(\lambda)$ and $P_{ii}^i(\Theta,\lambda)$ represent optical properties of ith homogeneous layer of the atmosphere. It should be noted that in AERONET retrieval algorithm (Dubovik and King, 2000) the accountancy for aerosol vertical variability is also possible. However, the sensitivity studies by Dubovik et al. (2000) show practically no sensitivity to aerosol vertical profile and, as a result, the operational AERONET retrievals are conducted under the assumption of vertically homogeneous atmosphere. The PARASOL aerosol retrieval by Dubovik et al. (2011) accounts for vertical variability of aerosol (similarly as shown in Eq. 8), and is designed to retrieve some information about aerosol vertical distribution. However, the passive radiometric and polarimetric observations from space have very moderate sensitivity to aerosol vertical variability. Therefore, vertical profiles of aerosol concentrations $c_k(h)$ in PARASOL algorithm are approximated

AMTD
6, 2253–2325, 2013

by the normal distribution and only median height of aerosol layer h_a is retrieved. In contrast, the profiles $c_k(h)$ in the present study are not approximated by any specific function and could have practically arbitrary shapes. Such approach is necessary for adequate modelling of lidar observations. In principle, such accurate accounting for aerosol vertical variability in radiative transfer calculations is not necessary for processing of passive observations, however, this may have some positive effects once radiometric data are combined with lidar observations, as it was done in this study.

3.2 Adjustments of the "forward model" to model lidar observations

Theoretically, the profiles $c_k(h)$ should describe the variability of aerosol at all altitudes from ground to space. However, the height range of lidar measurements has limitations. Usually ground-based lidar measurements do not cover all atmosphere altitudes and are conducted between the upper h_{max} and the lower h_{min} limits. Therefore, the vertical profiles $c_k(h)$ can be derived only between these limits and some assumptions about $c_k(h)$ for $h_{max} < h < h_{min}$ should be made in order to describe the vertical distribution of aerosol in the whole atmosphere column which is required for radiative transfer calculations. Here, the aerosol over h_{max} was assumed exponentially decreasing from $c_k(h_{max})$ to a value close to zero (10^{-30}) on the top of the atmosphere h_{TOA}, and under h_{min} it was assumed constant and equal to the last measured point $c_k(h_{min})$ as following:

$$c(h) = c(h_{min}), h \le h_{min}$$
$$c(h) = c(h_{max})\exp(-\alpha h), h > h_{max} \quad (12)$$

where α is chosen from the condition that $c_k(h_{TOA}) \to 0$.

The actual lidar observations used in the present study had an altitude range from 0.5 km up to 10 km, with the altitude resolution Δh of 15 m, which provides information about aerosol backscatter properties in $N_h \simeq 600$ altitude points h_i. In order to avoid excessively high number of the retrieved parameters in the algorithm N_h was limited to a smaller number (60). Since air density decreases exponentially and similar

AMTD
6, 2253–2325, 2013

scale is expected for the variability of aerosol profiles, the logarithmically equidistant ($\Delta \ln h = \text{Const}$) h_i have been chosen for describing profiles $c_k(h)$ in the algorithm.

The lidar measurements $L(\lambda, h)$ were also scaled down from $N_h \simeq 600$ to a smaller number. This decreases calculation time, and in addition, helps to decrease the effect of high frequency noise. Since the power of the laser pulse during lidar sounding decreases as square of the distance the level of noise strongly increases with the altitude. Therefore, the decimation of lidar signal in logarithmic scale over altitude provides practically useful noise suppression. Since lidar signal is measured with constant vertical resolution ($\Delta h = \text{Const}$), the decimation in logarithmic scale results in a decrease of sampling rate with the increase of altitude. According to the Kotelnikov-Nyquist theorem (Nyquist, 1928; Kotelnikov, 1933) the lower sampling rate at high altitudes decreases the amplitudes of high frequency oscillations, which usually are attributed to noise. The described decimation method could be considered as expanding sliding window low pass filter, allowing efficient noise suppression without loss of significant information about aerosol vertical structure.

3.3 The calibration of lidar signal

Commonly, retrievals use the attenuated backscatter (Eq. 1) normalized by attenuated backscatter at the reference altitude h_{ref}. This reference altitude is chosen under the assumption, that amount of the aerosol over that altitude is negligible, i.e.

$$L(\lambda, h_{\text{ref}}) = \beta_{\text{mol}}(\lambda, h_{\text{ref}}) \times \exp\left(-2\left(\tau^{\text{aer}}(\lambda) + \int_{h_0}^{h_{\text{ref}}} \left(\sigma_{\text{gas}}\left(\lambda, h'\right) + \sigma_{\text{mol}}\left(\lambda, h'\right)\right) \mathrm{d}h'\right)\right) \quad (13)$$

Correspondingly if $\tau^{\text{aer}}(\lambda)$ is known the above attenuated backscattering at the reference altitude h_{ref} can be easily calculated. However, due to the high presence of the noise at high altitudes the selection of the reference point remains a manual procedure that influences lidar retrievals (Kovalev and Oller, 1994; Matsumoto and Takeuchi, 1994). To address this problem Chaikovsky et al. (2004) has introduced “calibration

AMTD
6, 2253–2325, 2013

coefficient" $A(\lambda)$ in Eq. (1) and included this value into the set of the retrieved parameters. If error is small $A(\lambda) \to 1$. Here we follow the same concept and derive $A(\lambda)$ together with the other unknowns (see the list of the retrieved parameters in Table 1).

4 "Numerical inversion" organization

The retrieval is organized as multi-term LSM (Least-Square-Method) fitting similarly to the previous developments (Dubovik and King, 2000; Dubovik, 2004; Dubovik et al., 2011). This approach has shown to be convenient for designing efficient inversion of combined complex data sets (Sinyuk et al., 2007; Gatebe et al., 2010). This approach considers an inversion as statistically optimized simultaneous solution of a system of several independent equations:

$$f_k^* = f_k(a) + \Delta_k \ (k = 1, 2, ..., N_k) \tag{14}$$

where f_k^* are data from different sources i.e. f_k^* are the estimations of the characteristics $f_k(a)$. Since these estimations are originated from different sources their errors Δ_k are independent. Correspondingly, under the assumption of the Gaussian distribution of errors Δ_k the optimum solution is provided by multi-term LSM corresponding to a minimum of the quadratic form $\Psi(a)$ defined as:

$$2\Psi(a) = \sum_{k=1}^{N_k} \left(f_k^* - f_k(a)\right)^T \mathbf{C}_k^{-1} \left(f_k^* - f_k(a)\right) \to \min \tag{15}$$

where $\mathbf{C}_k$ are covariance matrices of the errors Δ_k . According to the suggestion of earlier studies (Dubovik and King, 2000, etc.) the above condition can be conveniently reformulated using weighting matrices $\mathbf{W}_k = \frac{1}{\varepsilon^2_k}\mathbf{C}_k$ (ε_k^2 is the first diagonal element of $\mathbf{C}_k$):

$$2\Psi(a) = \sum_{k=1}^{N_k} \frac{\varepsilon_0^2}{\varepsilon_k^2} \left(f_k^* - f_k(a)\right)^T \mathbf{C}_k^{-1} \left(f_k^* - f_k(a)\right) \to \min \tag{16}$$

AMTD
6, 2253–2325, 2013

where ε_0^2 is first diagonal element of $\mathbf{C}_{k=1}$ – covariance matrix of data set corresponding to $k = 1$. Correspondingly, the contribution of each term in Eq. (16) is scaled by the ratios of error variances $\frac{\varepsilon_0^2}{\varepsilon_k^2}$. As outlined by Dubovik and King (2000) this coefficient can be considered as Lagrange multiplier used in the constrained inversion techniques. In addition, in a case of noise properties assumed correctly, the achieved minimum can be used for estimating ε_0^2 as:

$$\left(\Psi(\mathrm{a})\,\varepsilon_0^2\right)_{\min} \to \varepsilon_0^2 \tag{17}$$

Additionally, in previous studies (Dubovik and King, 2000; Dubovik, 2004; Dubovik et al., 2011) the data both obtained from actual observations and from a priori knowledge are considered equally in equation system (Eq. 14). Such consideration allows convenient interpretation of a priori constraints and development of flexible retrieval formalism with use of multiple constraints. Specifically, for the convenience of interpretation of the present algorithm, the quadratic form (Eq. 16) can be represented by two terms:

$$2\left(\Psi(\mathrm{a})\,\varepsilon_0^2\right) = \sum_{k=1}^{N_{\mathrm{meas}}} \frac{\varepsilon_0^2}{\varepsilon_k^2}\left(\mathrm{f}_k^* - \mathrm{f}_k(\mathrm{a})\right)^T \mathbf{W}_k^{-1}\left(\mathrm{f}_k^* - \mathrm{f}_k(\mathrm{a})\right)$$

$$+ \sum_{p=1}^{N_{\mathrm{prior}}} \frac{\varepsilon_0^2}{\varepsilon_p^2}\left(s_p^* - s_p(\mathrm{a})\right)^T \mathbf{W}_p^{-1}\left(s_p^* - s_p(\mathrm{a})\right) \tag{18}$$

Here, the first group unites N_{meas} sets of independent measurements (with different level of accuracies) and the second unites N_{prior} sets of known a priori data sets used as a priori constraints. The measurements group has $N_{\mathrm{meas}} = 5$ and includes ($i = 1$) – AERONET spectral and angular measurements of atmospheric sky-radiances, ($i = 2$) – AERONET spectral measurements of aerosol optical thickness and ($i = 3, \ldots, 5$) –

AMTD
6, 2253–2325, 2013

lidar spectral measurements of attenuated backscatter. Thus, compared to AERONET retrieval (Dubovik and King, 2000) the measurement group in Eq. (18) includes additional terms corresponding to the measurements of attenuated backscatter at different wavelengths.

It should be noted that in many practical situations the observations are uncorrelated and provide equally accurate data, i.e. weighting matrices are equal to unity matrices $\mathbf{W}_k = \mathbf{I}$. Such weight matrix structure directly applicable to the passive measurements both for sky-radiances and aerosol optical thickness performed at different wavelengths. However such estimations that were implied in AERONET and POLDER retrievals, are not applicable to lidar measurements, as their variances depend both on the altitude and on the wavelength. Thus the weight matrix of lidar measurement will have a form of diagonal matrix that describes relative altitude dependence of variance for the given spectral channel:

$$\mathbf{W}_{\lambda_{\dots}} = \frac{1}{\varepsilon^2_{\lambda_{\dots}}} \begin{pmatrix} C_{\lambda_{\dots}}(h_{\min}) & 0 & 0 \\ 0 & \ddots & 0 \\ 0 & 0 & C_{\lambda_{\dots}}(h_{\max}) \end{pmatrix} \tag{19}$$

where $\varepsilon^2_{\lambda_{\dots}}$ is the minimum diagonal element of covariance matrix $\mathbf{C}_{\lambda_{\dots}}$ whose elements are defined similar with the approach proposed for LiRIC (Chaikovsky et al., 2006a; Denisov et al., 2006; Chaikovsky et al., 2012):

$$C_{\lambda_j}(h_i) = \omega^2 + \frac{g^2 + q^2 P^*(h_i, \lambda_j)}{AM\left(P^* - B^*(\lambda_j)\right)^2} + \frac{u^2}{\left(P^* - B^*(\lambda_j)\right)^2} + 4{\alpha_1}^2 + 4{\alpha_2}^2 \tag{20}$$

Where $P^*(\lambda_j, h_i)$ is recorded during lidar measurements, $B^*(\lambda_j)$ is background noise estimation, A is the accumulation of the signal, M is the number of the lidar signal counts in the altitude-averaging interval, g is the total deviation of the dark current and noise in receiving channel, q is the index that characterizes fluctuation noise

AMTD
6, 2253–2325, 2013

of the photo receiver and could be estimated on dark measurements of the photo-receiving module, u is the coefficient that characterizes the amplitude of synchronous noise in receiving channel, v is the non-linearity parameter; α_1, α_2 are the relative errors of molecular optical thickness and backscatter coefficient estimations. Parameters g, q, u, v are system dependent and estimated from testing of the lidar registration system and parameters α_1, α_2 are known for the used model of molecular atmosphere (Fleming et al. (1988), http://ccmc.gsfc.nasa.gov/modelweb/atmos/cospar1.html). The second group in Eq. (18) unites N_{prior} sets of known a priori derivatives of the aerosol characteristics. Specifically, we used the derivatives of retrieved size distributions $\mathrm{d}V_{f,c}(r)/\mathrm{d}\ln r$, the complex refractive indices spectral dependencies $n_{f,c}(\lambda)$, $k_{f,c}(\lambda)$ and the vertical variability of profiles $c_{f,c}(h)$. In order to avoid unrealistic oscillations of retrieved aerosol parameters, we assume that a priori values of s_{p} are zeros, i.e. $s_{\text{p}}^{*} = 0$ and Eq. (18) can be written as:

$$2\left(\Psi(\mathrm{a})\,\varepsilon_0^2\right) = \sum_{k=1}^{N_{meas}} \frac{\varepsilon_0^2}{\varepsilon_k^2}\left(\mathrm{f}_k^{*} - \mathrm{f}_k(\mathrm{a})\right)^T \mathbf{W}_k^{-1}\left(\mathrm{f}_k^{*} - \mathrm{f}_k(\mathrm{a})\right) + \sum_{p=1}^{N_{\text{prior}}} \frac{\varepsilon_0^2}{\varepsilon_k^2}\mathrm{a}\mathbf{S}_p^T\mathbf{S}_p\mathrm{a}^T \qquad (21)$$

here matrix $\mathbf{S}_p$ represents coefficients for calculating finite differences used to estimate the derivatives. The explicit form of these matrices is given in Dubovik (2004) and Dubovik et al. (2011). Thus, compared to the AERONET algorithm the a priori constraint group uses limitations on the derivatives of vertical profiles of aerosol concentrations. In addition, in the present algorithm we use the limitation on the derivatives separately for $\mathrm{d}V_{f,c}(r)/\mathrm{d}\ln r$, $n_{f,c}(\lambda)$ and $k_{f,c}(\lambda)$ for both fine and coarse modes. As a result, the algorithm used $N_{\text{prior}} = 8$ complementary a priori constraints.

It should be noted that limitations of the derivatives of the vertical profiles appears to be rather useful and very logical approach to avoid unrealistic spiky vertical variations in profiling that is also used in the LiRIC algorithm by Chaikovsky et al. (2002) Surprisingly, such apparently natural constraining is rarely used in profiling techniques (with few exceptions: Dubovik et al., 1998; Oshchepkov et al., 2002). For example, even the

AMTD
6, 2253–2325, 2013

cornerstone methodological studies of atmosphere profiling (e.g. Rodgers, 1976) propose limiting directly the values of profile using a priori estimations. Such approach is generally rather restrictive and can lead to the notable biases in the retrieval in the case when a priori assumed profiles are significantly different from the real ones. For example, in the aerosol microphysical applications where aerosol size distributions are retrieved from the measurements of spectral and angular scattering such approach appears to be unfruitful. Indeed, the shape and magnitudes of aerosol size distribution may strongly vary and direct restriction of its magnitude by a priori values is too restrictive. As a result, although the use of a priori estimates as a constrain in the retrieval of size distribution was proposed and tried by Twomey (1963) much earlier than in atmospheric profiling (e.g. Rodgers, 1976) it was never widely used. Instead, most of established aerosol retrieval algorithms (e.g. King et al., 1978; Nakajima et al., 1983, 1996; Dubovik et al., 1995; Dubovik and King, 2000, etc.) use the limitations of derivatives of aerosol size distribution. Such limitation are obviously more universal and do not have apparent dependence on aerosol type, loading, etc. The same property of derivatives constraining seems to be very advantageous for constraining vertical profile retrievals (as it was done in the present work).

The actual minimization of Eq. (21) in the present algorithm is performed in exactly the same way as described by Dubovik et al. (2011) for "single-pixel" retrieval scenario.

5 GARRLiC algorithm functionality and sensitivity tests

Series of sensitivity tests have been performed to verify the performance of the developed algorithm and to provide illustration of capabilities and limitations of the algorithm to derive a set of aerosol parameters (see Table 1) from coincident lidar and sun-photometer observations.

The sensitivity tests had been designed to conform with realistic conditions of each of the measurement. The tests were carried out for two cases representing situations when desert dust is mixed with urban pollution and biomass burning aerosols. Six

AMTD
6, 2253–2325, 2013

different scenarios were considered for the each mixture. Among them 3 scenarios were performed for high aerosol loading with total AOT of $\tau_a^{0.532} = 1$ and 3 with very low AOT of $\tau_a^{0.532} = 0.05$ at $\lambda = 0.532\,\mu m$. These two situations where chosen from the following considerations. At the high aerosol loading we expect that synergetic retrieval would maximally benefit from information from radiometric observations, while at very low AOT, the lidar data should provide maximum benefits. Indeed, the accuracy of AERONET retrievals is generally higher at high aerosol loading and significantly falls at very low AOT (Dubovik et al., 2000). In contrast, the lidar data remain reliable even at low aerosol loadings. For both high and low aerosol loading cases, three different cases of fine/coarse mode partition were modelled: $\tau_f/\tau_c = 4$, $\tau_f/\tau_c = 1$ and $\tau_f/\tau_c = 0.25$.

For each of the 6 scenarios, two series of the tests were made: (i) tests to estimate the sensitivity to random noise were made without any noise added and with random noise added to the simulated measurements, and (ii) tests to illustrate the possible improvements introduced by using both radiometric and lidar measurements in comparison with the standard AERONET inversion.

5.1 Description of aerosol and noise models used for sensitivity study

Two log-normal size distributions were used to generate 25 size bins (10 for fine and 15 for coarse aerosol modes). To make the size distributions directly comparable with actual AERONET observations the values of the generated bin radii were chosen corresponding to the ones of the standard AERONET retrieval. The values used to model size distributions of fine and coarse modes (see Table 2) were taken from AERONET retrieval climatology corresponding to desert dust and biomass-burning aerosols (Dubovik et al., 2002a).

The values of complex refractive indices at $\lambda = 0.44, 0.67, 0.87$ and $1.02\,\mu m$ for "urban pollution", "biomass burning" and "desert dust" aerosol models were adapted from actual long-time observation statistics over the GSFC, Banizombou and Solar Village AERONET sites correspondingly, where the listed types of the aerosols usually dominate in aerosol load (Dubovik et al., 2002a). The values for spectral channels

AMTD
6, 2253–2325, 2013

$\lambda = 0.355, 0.532$ and $1.064\,\mu m$ corresponding to lidar measurements were obtained by the extrapolation.

Two realistic scenarios with clear vertical separation of fine and coarse aerosol components were used. The fine mode was assumed to represent the background aerosol with specific vertical distribution, while coarse mode distribution had a thick layer approximately at 3 km. Both modes had significant amount of aerosol in the layers close to the ground to mimic the properties of the boundary layer. Both distributions had monotonous decrease over the altitude.

The values of the complex refractive indices as well as vertical distribution profiles of the aerosol models could be found marked as "TRUE" in Figs. 3–4 and 7.

To model realistic measurement conditions the random normally distributed noise was added to the generated measurements. The variance of noise in optical thickness measurement was set as 0.005, and the variance of noise in scattered irradiance was chosen as 3 %, i.e. $\frac{\Delta I}{I} = 0.03$; spectral and altitude dependent variances of lidar measurements were defined as

$$\frac{\Delta L(\lambda, h)}{L(\lambda, h)} = \varepsilon(\lambda)\, n(h) \tag{22}$$

where $\varepsilon(\lambda) = 0.2, 0.15, 0.1$ for $\lambda = 0.355, 0.532$ and $1.064\,\mu m$ correspondingly, and vertical dependence was set as the following function:

$$\begin{aligned} n(h) &= 1, \log(h) < 1 \\ n(h) &= \log(h), \log(h) \geq 1 \end{aligned} \tag{23}$$

Using above described microphysical model the synthetic AERONET and lidar measurements were simulated and then inverted. The results were compared with the "assumed" properties.

5.2 Sensitivity test results

The discussion of the sensitivity study results will focus on the retrievals of the aerosol properties that were not part of the standard AERONET inversion. Specifically, we will

AMTD
6, 2253–2325, 2013

pay particular attention to the retrieval of aerosol vertical profiles and differentiation between the properties of fine and coarse aerosol mode parameters including complex refractive indices, size distributions, etc. In addition we would like to note that the accuracy of aerosol size distribution retrieval is not discussed here. The results of our sensitivity tests show generally very similar tendencies as observed in earlier studies by Dubovik et al. (2000).

The results of the sensitivity tests are presented in Figs. 3–8. These results show that algorithm derives all aerosol parameters with good accuracy, and clearly distinguishes both aerosol modes. The addition of the realistic random noise did not dramatically affect the retrieval results, although once noise is added the retrieval results depart further from the "assumed" values.

Figures 3–5 show the retrievals of the aerosol complex refractive indices of each aerosol component under noisy conditions performed for 6 different AOT and obtained for two aerosol mixtures listed above. As it is seen in Figs. 3–5 method shows higher accuracy of columnar property retrieval in cases with higher aerosol loadings. Similar tendency is observed for the retrieval of vertical profiles.

Another observed trend is that the accuracy of the retrievals of complex refractive index for each aerosol mode strongly correlates with the contribution of this mode to the signal. Specifically, two following tendencies are observed. First, the higher the presence of the mode, the better retrieval accuracy of the refractive index for this mode. Second, the retrieval error of the refractive index increases from shorter wavelengths to longer ones for the fine mode, and for the coarse mode the tendency is opposite.

Figure 6 illustrates that similar tendency is observed for the retrievals of the single scattering albedo.This trend is especially evident in the situations with low total AOT and when of one of the components dominates. As can be seen from Fig. 6, in such situation retrieval errors of the properties of minor aerosol mode become unacceptably high. This leads to incorrect separation of the total single scattering albedo between these two aerosol components at shorter wavelengths. The retrievals of total single scattering albedo depend on the total optical thickness similarly as observed by

AMTD
6, 2253–2325, 2013

(Dubovik et al., 2000). The scenario with high total AOT and equal partition between the modes is the most favourable for overall retrieval.

Figure 7 shows the retrievals of the vertical distributions. As can be seen form these plots the algorithm gives generally adequate vertical profiles for both modes. At the same time, it tends to slightly overestimate the amount of the fine mode and to underestimate coarse mode content in the layers that contain the mixture of aerosols of both types. However, the algorithm always provides adequate total extinction estimations for the given layer (see Fig. 8).

This tendency remains even in noise free conditions. It probably can be explained by insufficient information content for perfect separation of fine and coarse mode contributions to the total lidar signal in the mixed layers.

Figure 8 illustrate the algorithm capability to retrieve vertical distributions of basic aerosol optical properties such as extinction, absorption, single scattering albedo and lidar ratio both in noise free conditions and with random noise added. The figures show the retrievals for equally mixed dust and smoke fractions in a sense that $\tau_{smoke} = \tau_{dust} = 0.5$. Figure 8 demonstrates that the errors in estimations of single scattering albedo and lidar ratios are generally higher compared to the errors of extinction and absorption.

Another tendency observed in the sensitivity study is lower sensitivity of the retrieval to the fine mode properties, especially to the complex refractive index. These high errors in derived complex indices of refraction propagate to the estimations of other optical properties of fine mode. The trend remains even in situations with high aerosol loading in noise free conditions. Figure 9 shows that fundamental reason for this feature is a selective sensitivity of the lidar measurement to the optical properties of the particles of different size and shape. Specifically, Fig. 9 indicates that lidar ratio of the fine mode is less affected by the changes in refractive index compared to the coarse mode. This could be explained by smaller sensitivity of light scattering to the particle shape of the fine mode that is well illustrated by Fig. 9, showing stronger dependence of the lidar ratio on complex refractive index for the spherical particles of coarse mode. Therefore,

AMTD
6, 2253–2325, 2013

since lidar measurements are sensitive mainly to lidar ratio, lidar measurements do not provide significantly new information about refractive index of fine mode.

Also at shorter wavelengths the high molecular scattering reduces the aerosol contribution to the lidar signal. This also leads to decrease of the sensitivity to the fine mode aerosol properties since a significant part of information about fine fraction relies namely on shorter wavelengths.

It should be noted that a number of studies (Mishchenko et al., 2000, 2004; Dubovik et al., 2006) indicate high sensitivity of polarimetric passive measurements to the refractive index of the fine mode. Therefore, usage of radiometers with polarimetric capabilities could potentially result in better retrievals of the aerosol parameters of the fine mode.

5.3 Improvements introduced by joint inversion of lidar and AERONET

A synergetic handling of co-incident radiometer and lidar data is obviously beneficial for acquisition of improved vertical characterization of aerosol. The processing of lidar data always relies on assumptions about some aerosol properties. Obtaining this missing information from nearby radiometer is evidently preferable to a simple assumption of these properties from climatologies. Therefore, the positive influence of the radiometer data on the lidar retrievals was emphasized in a number of previous studies (Chaikovsky et al., 2006c; Cuesta et al., 2008). However, all previous radiometer-lidar synergy approaches used AERONET retrievals in the form of a priori assumptions for improving lidar retrievals. GARRLiC is the first development trying to explore possibility of improving AERONET retrieval by using extra information of co-located lidar observations. The possibility to distinguish indices of the refraction of fine and coarse particles is one of the most significant innovations proposed by GARRLiC, since it was not achievable using only AERONET data as shown in studies by Dubovik et al. (2000). The results of sensitivity tests presented in previous section showed the achievable levels of retrieval accuracy of the complex refractive index using both lidar and radiometer data. At the same time, it is clear that the lidar data provide additional information about

AMTD
6, 2253–2325, 2013

aerosol properties because of high sensitivity of lidar data to aerosol lidar ratio. Therefore, in order to provide additional illustration of positive effect from using lidar data on aerosol columnar properties, we analyse the changes in accuracy of the retrieval of lidar ratios by adding lidar data to AERONET observations. Also any improvement in lidar ratio estimations brings straightforward enhancements in retrieval of vertical profiles of aerosol concentrations.

With a purpose to access and illustrate possible improvements in the retrieval of aerosol columnar properties, additional scenario was added to the sensitivity study: inversion, neglecting the measurements provided by lidar. Figure 10 shows the comparisons of errors of lidar ratio retrievals conducted for AERONET data only and for a combination of AERONET and lidar. The results demonstrate that joint retrieval allows more accurate retrievals of lidar ratio for both aerosol components in such challenging cases when one mode dominates in optical thickness. In such cases retrieval without lidar measurements tends to estimate all properties of both modes close to those of dominating one, leading to dramatic errors in lidar ratio estimations. The errors of the retrieval of the dominating mode lidar ratio remain almost the same for both inversion strategies. These results lead to a conclusion that supplementing radiometer data by lidar observations helps to improve the retrieval of aerosol properties of minor mode in the aerosol mixture. Consequently, the retrieval of vertical profile of the minor mode concentration is also should be more accurate compared to the retrievals by the approaches of Chaikovsky et al. (2006c) and Cuesta et al. (2008) which assume lidar ratios from AERONET retrievals.

Also, based on the observations made from Fig. 9 that lidar ratio is very sensitive to the retrieval accuracy of spherical particles faction, we have evaluated the possible improvements in the retrieval of this parameter by using joint inversion of AERONET and radiometer data.

Table 3 summarizes the relative errors of retrieval of this parameter for three cases of aerosol with different partition of aerosol modes. The results were obtained for high aerosol load within three inversion scenarios: the joint inversion of radiometer and lidar

AMTD
6, 2253–2325, 2013

data without any noise added; the joint inversion with random noise added to the data and the inversion of radiometer data only with random noise added to the observations. Although without information about polarization the sensitivity to this parameter is quite low and depends on aerosol optical thickness, the fact that backscatter depends on this parameter (see Fig. 9) allows decreasing retrieval errors in the situations when coarse mode dominates in optical thickness. As it is seen from the Table 3, the absence of lidar data in the presence of the random noise makes accurate GARRLiC retrieval of this parameter impossible even in situation with significant amount of coarse mode, while in the presence of lidar data sensitivity to this parameter remains for the same case of aerosol load.

Decrease of retrieval error with growth of the coarse mode concentration is explained by higher sensitivity of the measurements to the shape parameters of bigger particles.

The analysis of test results allows making a conclusion that being supplied with sufficient measurement information combined inversion could provide deep synergy of two different types of aerosol remote sensing, resulting in more accurate and qualitative retrievals compared to the single instrument inversions.

6 GARRLiC applications to real lidar/sun-photometer observations

The algorithm has been applied to lidar/sun-photometer measurements collected at observation site of the Laboratory of Scattering Media at Institute of Physics, Minsk, Belarus. Station is equipped by standard AERONET sun-photometer and several multi-wavelength lidars that provided measurements of attenuated backscatter at 0.355, 0.532 and 1.064 µm.

Parameters that characterize noise (Eq. 20) in these lidar systems were estimated as shown in Table 4.

Two typical situations were chosen to illustrate the inversion results: (i) the observation of dust outburst from Sahara desert transported over Minsk on 2 June 2008, (ii) observation on 13 August 2010 of smoke plum transported from Russian forest

AMTD
6, 2253–2325, 2013

fires over East Europe. Figures 11–12 show the atmosphere back trajectories provided for Minsk AERONET site (http://croc.gsfc.nasa.gov/aeronet/, Schoeberl and Newman (1995); Pickering et al. (2001)) for these cases. The analysis of these back trajectories illustrates that air masses from mentioned regions should be present over Minsk during measurement periods.

Figures 13–14 present the retrieved aerosol columnar microphysical properties and Figs. 16 and 17 show the retrieved columnar optical parameters all in comparison with standard AERONET retrievals for this site. Figures 15 and 18–20 present the retrieved vertical profiles of microphysical and optical aerosol properties. Figures 21 and 22 are dedicated to qualifications of the vertical retrievals, Fig. 21 presents the comparison of GARRLiC results with LiRIC retrievals made for the same measurements and Fig. 22 presents achieved fits of the lidar measurements.

Retrieved size distributions (Fig. 13) are consistent with the expectations for observed aerosol types: domination of fine mode for smoke and of coarse mode for desert dust. Both retrievals show good agreement with AERONET retrievals, the difference in the fine mode retrievals between two methods in the dust observation case could probably be explained by lower sensitivity of the AERONET inversion to minor aerosol modes.

The retrieved refractive indices (Fig. 14) are clearly distinguished between modes and are coherent with the values expected for these aerosol types: highly absorbing fine mode for smoke, real part of refractive index for coarse mode close to the observations of this parameter for dust (Dubovik et al., 2002a). Since, the AERONET retrieval does not discriminate the refractive index of the modes, the AERONET derived values can not be compared directly to the GARRLiC retrieval. Nonetheless, it is clear that there is logical agreement between two retrievals since AERONET derived refractive indices are generally in the middle between values of fine and coarse modes obtained by GARRLiC.

The vertical distributions of fine and coarse modes (Fig. 15) clearly discriminate the vertical structure of the aerosols of different types. Both retrievals agree well with

AMTD
6, 2253–2325, 2013

back-trajectory analysis: according to Figs. 11 and 12 the atmospheric layer from the region of forest fires was expected at the altitude across 2 km, and the layer from Sahara desert was expected around 4 km. Retrievals of lidar ratios shown in Fig. 16 demonstrate notable differences between AERONET and GARRLiC values. The main difference is located at shorter wavelengths. These differences are probably caused by the significant differences in the sensitivities of both data sets, and by the differences in assumptions. Specifically, AERONET radiometer does not include observations in backscattering direction, and assumption of size independent refractive index may also result in an additional error in the lidar ratio estimation. For example, in Fig. 9 the high values of absorption for the coarse mode in AERONET retrieval, that could be caused by the presence of smoke in the mixture, lead to unnatural lidar ratios retrieved for the desert dust (see for e.g. Cattrall et al., 2005).

The spherical particles faction retrieved for these two cases gave 40 % of spherical particles for the smoke event and 25 % for the dust, compared to the 99 % and 2 % from AERONET retrievals. This difference can be explained by high sensitivity of the lidar measurements to backscatter from non-spherical particles (see Dubovik et al., 2006 and Fig. 9).

Figure 17 illustrates the retrievals of columnar single scattering albedo. Total (i.e. mixture of fine and coarse) SSA shows good agreement with AERONET retrievals and with climatological values (Dubovik et al., 2002a). Both spectral dependencies of smoke and dust single scattering albedos were retrieved. The total single scattering albedo is closer to the value of dominating aerosol mode for both retrievals.

Figures 18–20 demonstrate the vertical distributions of single scattering albedos, lidar ratios and extinction calculated using retrieved parameters at the wavelengths of lidar measurements. All distributions have noticeable vertical structure that agrees with the retrieved vertical distributions of aerosol concentrations. Both values of single scattering albedo and lidar ratios at all single layers are in the ranges of typical values for dust and smoke aerosols (Dubovik et al., 2002a; Cattrall et al., 2005). It should be noted, that the particular behaviour of profiles in Fig. 18–19 at higher altitudes could

AMTD
6, 2253–2325, 2013

be explained by a very small amount of the aerosol present in the upper atmosphere layers and very weak signal returned from this altitude range.

Figure 21 shows vertical distributions retrieved by the GARRLiC compared with the results of LiRIC inversion (Chaikovsky et al., 2012) made for the same measurement set during dust event. Both retrieved profiles are in good agreement. The minor differences could be explained by smaller amount of altitude layers in the GARRLiC retrieval and differences in lidar ratios estimations for both modes. Such high similarity could be explained by the small (see Fig. 14) difference in complex refractive indices of fine and coarse aerosol modes, which should result in close values of derived lidar ratios, thus not causing any significant effect on the retrieved aerosol concentration profiles. Therefore, for the situations when the usage of the same values of complex refractive index for both aerosol modes could be justified, these two methods should provide similar results. We have observed that in less favourable situations AERONET estimates of lidar ratio can show more significant deviations, thus affecting the retrievals of vertical concentration profiles more drastically.

In Fig. 22 lidar measurements fits achieved during GARRLiC inversions are presented. Since both measurements were made with different duration, the noise at higher altitudes is much stronger in the case with smoke observations due to the smaller accumulation of the lidar signal. The use of lidar measurements down-sampling and application of additional smoothness constrains allowed us to diminish the influence of high noise and stabilize the retrievals in the presence of random noise. The misfits at shorter wavelengths that could be observed at lower altitudes in the part of Fig. 22 referring to the dust observation are caused by the non-uniform overlap of the fields of view of receiver and emitter of the lidar system.

Thus, the results of GARRLiC application to real data and their comparisons with AERONET and LiRIC retrieval results showed an encouraging agreement for both columnar and vertical properties of aerosol. At the same time, the GARRLiC retrieval differentiates between columnar optical properties of fine and coarse modes of aerosol relying on additional information contained in lidar observations.

AMTD
6, 2253–2325, 2013

7 Conclusions

This paper has discussed in detail a concept for a new GARRLiC algorithm developed for deriving detailed properties of two atmospheric aerosol components from coincident lidar and photometric measurements. The algorithm is developed using the heritage of the AERONET, PARASOL and LiRIC algorithms. The algorithm is designed to invert the co-incident observations of CIMEL sun/sky photometer that registers direct and scattered atmospheric radiation at four wavelengths in up to 35 directions and multi-wavelength elastic lidar that registers backscattered radiation at three wavelengths in up to 1000 altitude layers. The algorithm derives an extended set of parameters for both columnar and vertical aerosol properties, including aerosol sizes, shape, spectral complex refractive index for both fine and coarse aerosol modes, as well as vertical profiles of mode concentrations.

The concept of the algorithm is aimed to achieve higher accuracy of the retrieval, since in such an approach the solution usually relying only on passive measurement of the radiometer is benefiting from information contained in coincident active observations by lidar and method uses a smaller number of assumptions about aerosol. The paper provided detailed description of the full set of formulations necessary for realizing this concept.

The performance of the developed algorithm has been demonstrated by application to both synthetically generated and real coincident sun-photometer and lidar observations. First, a series of sensitivity tests were conducted by applying the algorithm to the synthetic sun-photometer and lidar observations for the cases of aerosol mixtures containing desert dust with urban pollution and biomass burning aerosols. The simulations were designed to mimic observations of real aerosol. With this purpose, aerosol models derived from AERONET observations in Solar Village (Saudi Arabia), African savanna (Zambia) and GSFC (Greenbelt, MD) were used to generate synthetic proxy measurements, both photometric and lidar. The data were perturbed by random noise before applying the retrieval algorithm. The results of the tests showed that the

AMTD
6, 2253–2325, 2013

complete set of aerosol parameters for each aerosol component can be robustly derived with acceptable accuracy in all considered situations. The better accuracy was observed for the higher aerosol load.

In addition, the GARRLiC algorithm was applied to coincident lidar and sun-photometer observations performed at Minsk (Belarus) AERONET site. The comparison of the derived aerosol properties with available observations by AERONET ground-based sun/sky-radiometers indicated encouraging consistency of microphysical parameters of aerosol components derived from joint inversion with those obtained by AERONET retrieval. More comprehensive studies for testing and tuning the developed algorithm including accountancy for polarization effects both for sun- photometer and lidar observations are planned in future efforts. Such important aspects of algorithm implementation as coincident measurements requirements are to be addressed in follow-on studies.

Described GARRLiC algorithm is not only limited by ground observations or by used instrument types. Presented concept could be adapted to a variety of aerosol remote sensing instruments available, including ground-based polarimetric measurements of both sun-photometers and lidars, Raman scattering lidars and spaceborne systems like PARASOL and CALIPSO, providing wider opportunities in global comprehensive aerosol characterization.

Acknowledgements. The authors are very thankful to AERONET for establishing and maintaining the sites used in this work. This research has been supported by the University of Lille, and Region Nord-Pas-de-Calais. A. Lopatin was supported by a CROUS/CNOUS fellowship of the French Government. The research leading to these results has received funding from the European Union Seventh Framework Program (*FP*7/2007–2013) under grant agreement No. 262254.

AMTD
6, 2253–2325, 2013

The publication of this article is financed by CNRS-INSU.

References

Adam, M., Pahlow, M., Kovalev, V. A., Ondov, J. M., Parlange, M. B., and Nair, N.: Aerosol optical characterization by nephelometer and lidar: The Baltimore Supersite experiment during the Canadian forest fire smoke intrusion, J. Geophys. Res., 109, D16S02, doi:10.1029/2003JD004047, 2004. 2258

Ahmad, Z., Franz, B. A., McClain, C. R., Kwiatkowska, E. J., Werdell, J., Shettle, E. P., and Holben, B. N.: New aerosol models for the retrieval of aerosol optical thickness and normalized water-leaving radiances from the SeaWiFS and MODIS sensors over coastal regions and open oceans, Appl. Opt., 49, 5545–5560, 2010. 2256

Ansmann, A., Riebersell, M., Wandinger, U., Weitkamp, C., Voss, E., Lahmann, W., and Michaelis, W.: Combined raman-elastic lidar for vertical profiling of moisture, aerosols extinction, backscatter and lidar ratio, Appl. Phys, 55, 18–28, 1992. 2257

Ansmann, A., Tesche, M., Groß, S., Freudenthaler, V., Seifert, P., Hiebsch, A., Schmidt, J., Wandinger, U., Mattis, I., Müller, D., and Wiegner, M.: The 16 April 2010 major volcanic ash plume over central Europe: EARLINET lidar and AERONET photometer observations at Leipzig and Munich, Germany, Geophys. Res. Lett., 37, L13810, doi:10.1029/2010GL043809, 2010. 2256

Ansmann, A., Tesche, M., Seifert, P., Groß, S., Freudenthaler, V., Apituley, A., Wilson, K. M., Serikov, I., Linné, H., Heinold, B., Hiebsch, A., Schnell, F., Schmidt, J., Mattis, I., Wandinger, U., and Wiegner, M.: Ash and fine mode particle mass profiles from EARLINET/AERONET observations over central Europe after the eruptions of the Eyjafjallajökull volcano in 2010, J. Geophys. Res., 116, D00U02, doi:10.1029/2010JD015567, 2011. 2259

Antuña, J., Andrade, M., Landulfo, E., Clemesha, B., Quel, E., and Bastidas, A.: B. Clemesha, E. Quel, A. Bastidas, Building a Lidar Network in Latin America: Progress and Difficulties, in 23rd International Laser Radar Conference, Nara, Japan, 24–28 July, 2006. 2256

Barker, J. and Tingey, D. T.: Air Pollution Effects on Biodiversity, Springer, New York, 1992. 2255

Bösenberg, J.: EARLINET-A European Aerosol Research Lidar Network, Advances in Laser Remote sensing, in: Selected papers 20th Int. Laser Radar Conference (ILRC), Vichy, France, 10–14 July 2000, 155–158, 2000. 2256

Bösenberg, J. and Hoff, R. M.: Plan for the implementation of the GAW Aerosol Lidar Observation Network GALION, WMO/TD-No. 1443 178, GAW, 2007. 2256

Bréon, F.-M.: How Do Aerosols Affects Cloudiness and Climate?, Science, 313, 623–624, doi:10.1126/science.1131668, 2006. 2256

Bréon, F. M., Buriez, J. C., Couvert, P., Deschamps, P. Y., Deuze, J. L., Herman, M., Goloub, P., Leroy, M., Lifermann, A., Moulin, C., Parol, F., Seze, G., Tanré, D., Vanbauce, C., and Vesperini, M.: Scientific results from the POLarization and Directionality of the Earth's Reflectances (POLDER), Adv. Space Res., 30, 2383–238, 2002. 2255

Cattrall, C., Reagan, J., Thome, K., and Dubovik, O.: Variability of aerosol and spectral lidar and backscatter and extinction ratios of key aerosol types derived from selected Aerosol Robotic network locations, J. Geophys. Res., 110, D10S11, doi:10.1029/2004JD005124, 2005. 2265, 2283

Chaikovsky, A. P., Dubovik, O., Holben, B. N., and Bril, A. I.: Methodology to retrieve atmospheric aerosol parameters by combining ground-based measurements of multiwavelength lidar and sun sky-scanning radiometer, in: Proceeding of Eight International Symposium on Atmospheric and Ocean and Ocean Optics: Atmospheric Physics, edited by: Zherebtsov, G. A., Matvienko, G. G., Banakh, V. A., and Koshelev, V. V., SPIE, 4678, 257–268, doi:10.1117/12.458450, 2002. 2259, 2273

Chaikovsky, A., Bril, A., Dubovik, O., Holben, B., Thompson, A., Goloub, P., O'Neill, N., Sobolewski, P., Bösenberg, J., Ansmann, A., Wandinger, U., and Mattis, I.: CIMEL and multiwavelength lidar measurements for troposphere aerosol altitude distributions investigation, long-range transfer monitoring and regional ecological problems solution: field validation of retrieval techniques, Óptica Pura y Aplicada, 37, 3241–3246, 2004. 2259

Chaikovsky, A., Bril, A., Denisov, S., and Balashevich, N.: Algorithms and software for lidar data processing in CIS-LiNet, in: Reviewed and Revised Papers Presented at the 23rd

AMTD
6, 2253–2325, 2013

International Laser radar Conference, 24–28 July 2006, Nara, Japan, edited by: Chikao Nagasava, N. S., 667–670, 2006a. 2259, 2272

Chaikovsky, A., Ivanov, A., Balin, Y., Elnikov, A., Tulinov, G., Plusnin, I., Bukin, O., and Chen, B.: Lidar network CIS- LiNet for monitoring aerosol and ozone in CIS regions, in: Proc. Twelfth Joint International Symposium on Atmospheric and Ocean Optics/Atmospheric Physics, edited by: Gelii A. Zherebtsov, G. G. M., 6160, 616035–616039, SPIE, doi:10.1117/12.675920, 2006b. 2256

Chaikovsky, A., Ivanov, A., Korol, M., Slesar, A., S., D., Osipenko, F., Hutko, I., Dubovik, O., Holben, B., and Goloub, P.: Atmospheric participate matter variability in an industrial center from multi-wavelength lidar and Sun-sky radiometer measurements, in: Proc. Twelfth Joint International Symposium on Atmospheric and Ocean Optics/Atmospheric Physics, edited by: Gelii A. Zherebtsov, G. G. M., SPIE, 6160, 61601Y–61601Y–12, doi:10.1117/12.675466, 2006c. 2279, 2280

Chaikovsky, A., Dubovik, O., Goloub, P., Tanré, D., Chaikovskaya, L., Denisov, S., Grudo, Y., Lopatsin, A., Karol, Y., Lapyonok, T., Korol, M., Osipenko, F., Savitski, D., and Slesar, A.: Combined lidar and radiometric sounding of atmospheric aerosol: algorithm of data processing, software, dissemination, in: Proceedings of XVIII International symposium “Atmospheric and ocean optics. Atmosphere physics”, Irkutsk, Russian Federation, 2–6 July, C1–C4, 2012. 2259, 2272, 2284

Charlson, R. J., Schwartz, S. E., Hales, J. M., Cess, R. D., Coakley, J. A., Hansen, J. E., and Hofmann, D. J.: Aerosols and global warming response, Science, 256, 598–599, 1992. 2255

Costa, M., Levizzani, V., and Silva, A. M.: Part II: Aerosol characterization and direct radiative forcing assessment over the ocean: Application to test cases and validation, J. Appl. Met., 43, 1818–1833, 2004. 2256

Cuesta, J., Flamant, H. P., and Flamant, C.: Synergetic technique combining elastic backscatter lidar data and sunphotometer AERONET inversion for retrieval by layer of aerosol optical and microphysical properties, Appl. Opt., 47, 4598–4611, 2008. 2259, 2279, 2280

D’Almeida, G. A., Koepke, P., and Shettle, E. P.: Atmospheric Aerosols: Global Climatology and Radiative Characteristics, p. 561, A. Deepak Pub., 1991. 2255

Denisov, S., Chaikovsky, A., Bril, A., and Balashevich, N.: Integrated software for lidar data processing, in: Proceedings Of International Workshop ISTC “Baikal 2006”, Monitoring of large-scale atmosphere changes in CIS regions: co-operation of the international measuring

AMTD
6, 2253–2325, 2013

networks AERONET, EARLINET, AD-Net, NDSC, as well as scientific groups in CIS, 15–19 August 2006, Irkutsk, Russia, 41–43, 2006. 2272

Di Girolamo, P., Summa, D., Bhawar, R., Di Lorio, T., Cacciani, M., Veselovskii, I., Dubovik, O., and Kolgotin, A.: Raman lidar observations of a Saharan dust outbreak event: Characterization of the dust optical properties and determination of particle size and microphysical parameters, J. Atmos. Environ., 50, 66–78, doi:10.1016/j.atmosenv.2011.12.061, 2012. 2265

Dubovik, O.: Optimization of Numerical Inversion in Photopolarimetric Remote Sensing, in: Photopolarimetry in Remote Sensing, edited by: Videen, G., Yatskiv, Y., and Mishchenko, M., 65–106, Kluwer Academic Publishers, Dordrecht, The Netherlands, 2004. 2261, 2270, 2271, 2273

Dubovik, O. and King, M.: A flexible inversion algorithm for retrieval of aerosol optical properties from Sun and sky radiance measurements, J. Geophys. Res., D16, 20673–20696, 2000. 2255, 2260, 2261, 2262, 2265, 2267, 2270, 2271, 2272, 2274

Dubovik, O., Lapyonok, T., and Oshchepkov, S.: Improved technique for data inversion: optical sizing of multicomponent aerosols, Appl. Opt., 34, 8422–8436, 1995. 2274

Dubovik, O., Yokota, T., and Sasano, Y.: Improved technique for data inversion and its application to the retrieval algorithm for adeos/ilas., Adv. Space Res., 21, 397–403, 1998. 2273

Dubovik, O., Smirnov, A., Holben, B. N., King, M., Kaufman, Y. J., Eck, T. F., and Slutsker, I.: Accuracy assessments of aerosol optical properties retrieved from Aerosol Robotic Network (AERONET) sun and sky radiance measurements, J. Geophys. Res., 105, 9791–9806, 2000. 2260, 2265, 2267, 2275, 2277, 2278, 2279

Dubovik, O., Holben, B., Eck, T., Smirnov, A., Kaufman, Y., King, M., Tanré, D., and Slutsker, I.: Variability of absorption and optical properties of key aerosol types observed in worldwide locations, J. Atmos. Sci., 59, 590–608, 2002a. 2260, 2275, 2282, 2283

Dubovik, O., Holben, B. N., Lapyonok, T., Sinyuk, A., Mishchenko, M. I., Yang, P., and Slutsker, I.: Non-spherical aerosol retrieval method employing light scattering by spheroids, Geophys. Res. Lett., 29(10), doi:10.1029/2001GL014506, 2002b. 2260, 2265

Dubovik, O., Sinyuk, A., Lapyonok, T., Holben, B. N., Mishchenko, M., Yang, P., Eck, T. F., Volten, H., Munoz, O., Veihelmann, B., van der Zande, W. J., Leon, J.-F., Sorokin, M., and Slutsker, I.: Application of spheroid models to account for aerosol particle nonsphericity in remote sensing of desert dust, J. Geophys. Res., 111, D11208, doi:10.1029/2005JD006619, 2006. 2260, 2265, 2279, 2283

AMTD
6, 2253–2325, 2013

Dubovik, O., Herman, M., Holdak, A., Lapyonok, T., Tanré, D., Deuzé, J. L., Ducos, F., Sinyuk, A., and Lopatin, A.: Statistically optimized inversion algorithm for enhanced retrieval of aerosol properties from spectral multi-angle polarimetric satellite observations, Atmos. Meas. Tech., 4, 975–1018, doi:10.5194/amt-4-975-2011, 2011. 2261, 2262, 2264, 2265, 2267, 2270, 2271, 2273, 2274

Eck, T. F., Holben, B. N., Dubovik, O., Smirnov, A., Goloub, P., Chen, H. B., Chatenet, B., Gomes, L., Zhang, X.-Y., Tsay, S.-C., Ji, Q., Giles, D., and Slutsker, I.: Columnar aerosol optical properties at AERONET sites in Central-eastern Asia and aerosol transport to the tropical mid Pacific, J. Geophys. Res., 110, 975–1018, doi:10.1029/2004JD005274, 2005. 2260

Eck, T. F., Holben, B. N., Reid, J. S., Giles, D. M., Rivas, M. A., Singh, R. P., Tripathi, S. N., Bruegge, C. J., Platnick, S., Arnold, G. T., Krotkov, N. A., Carn, S. A., Sinyuk, A., Dubovik, O., Arola, A., Schafer, J. S., Artaxo, P., Smirnov, A., Chen, H., and Goloub, P.: Fog- and cloud-induced aerosol modification observed by the Aerosol Robotic Network (AERONET), J. Geophys. Res., 117, D07206, doi:10.1029/2011JD016839, 2012. 2260

Fernald, F. G.: Analysis of atmospheric lidar observations – Some comments, Appl. Opt., 23, 652–653, 1984. 2258

Fernald, F. G., Herman, B. M., and Reagan, J. A.: Determination of aerosol height distributions by lidar, J. Appl. Meteorol., 11, 482–489, 1972. 2258

Ferrare, R. A., Melfi, S. H., Whiteman, D. N., Evans, K. D., Leifer, R., and Kaufman, Y. J.: Raman lidar measurements of aerosol extinction and backscattering 1. Methods and comparisons, J. Geophys. Res., 103, 19663–19672, 1998a. 2257

Ferrare, R. A., Melfi, S. H., Whiteman, D. N.and Evans, K. D., Poellot, M., and Kaufman, Y. J.: Raman lidar measurements of aerosol extinction and back- scattering 2. Derivation of aerosol real refractive index, single-scattering albedo, and humidification factor using Raman lidar and aircraft size distribution measurements, J. Geophys. Res., 103, 19673–19690, 1998b. 2257

Fleming, E., Chandra, S., Shoeberl, M., and Barnett, J.: Mean Global Climatology of Temperature, Wind, Geopotential Height, and Pressure for 0–120 km. NASA Technical Memorandum 100697, NASA, 1988. 2263, 2273

Forster, P., Ramaswany, V., Artaxo, P., Bernsten, T., Betts, R., Fahey, D. W., Haywood, J., Lean, J., Lowe, D., Myhre, G., Nganga, J., Prinn, R., Raga, G., Schulz, M., and Dorland, R. V.: Changes in atmospheric constituents and in radiative forcing, Climate Change 2007: the

AMTD
6, 2253–2325, 2013

physical science basis. Contribution of working group I to the fourth assessment report of Intergovernmental Panel on Climate Change, IPCC report, 2007. 2255, 2256
Gatebe, C. K., Dubovik, O., King, M. D., and Sinyuk, A.: Simultaneous retrieval of aerosol and surface optical properties from combined airborne- and ground-based direct and diffuse radiometric measurements, Atmos. Chem. Phys., 10, 2777–2794, doi:10.5194/acp-10-2777-2010, 2010. 2261, 2262, 2270
Gobbi, G. P., Barnaba, F., Van Dingenen, R., Putaud, J. P., Mircea, M., and Facchini, M. C.: Lidar and in situ observations of continental and Saharan aerosol: closure analysis of particles optical and physical properties, Atmos. Chem. Phys., 3, 2161–2172, doi:10.5194/acp-3-2161-2003, 2003. 2257
Gutkowicz-Krusin, D.: Multiangle lidar performance in the presence of horizontal inhomogeneities in atmospheric extinction and scattering, Appl. Opt., 32, 3266–3272, 1993. 2257
Hair, J., Hostetler, C., Cook, A., Harper, D., Ferrare, R., Mack, T., Welch, W., Izquierdo, L., and Hovis, F. E.: Airborne High Spectral Resolution Lidar for Profiling Aerosol Optical Properties, Appl. Opt., 47, 6734–6752, doi:10.1364/AO.47.006734, 2008. 2258
Hansen, J., Sato, M., Kharecha, P., and von Schuckmann, K.: Earth's energy imbalance and implications, Atmos. Chem. Phys., 11, 13421–13449, 2011, http://www.atmos-chem-phys.net/11/13421/2011/. 2255, 2256
Harrison, R. M. and Yin, J.: Particulate matter in the atmosphere: Which particle properties are important for its effects on health, Sci. Total Environ., 249, 85–101, 2000. 2255
Hasekamp, O. P., Litvinov, P., and Butz, A.: Aerosol properties over the ocean from PARASOL multiangle photopolarimetric measurements, J. Geophys. Res.-Atmos., 116, D14204, doi:10.1029/2010JD015469, 2011. 2256
Hobbs, P. V.: Aerosol-cloud interactions, in Aerosol-Cloud-Climate Interactions, 33–69, Academic, San Diego, Calif., 1993. 2255
Hoff, R. M., Wiebe, H. A., and Guise-Bagley, L.: Lidar, nephelometer, and in situ aerosol experiments in southern Ontario, J. Geophys. Res., 101, 19199–19209, 1996. 2258
Holben, B.: AERONET-A federated instrument network and data archive for aerosol characterization, Remote Sens. Environ., 66, 1–16, 1998. 2256
Holben, B., Eck, T., Schafer, J., Giles, D., and Sorokin, M.: Distributed Regional Aerosol Gridded Observation Networks (DRAGON), White Paper, 2011. 2256
Jones, A. P.: Indoor air quality and health, Atoms. Environ., 33, 4535–4564, 1999. 2255

AMTD
6, 2253–2325, 2013

Kahn, R. A., Gaitley, B. J., Garay, M. J., Diner, D. J., Eck, T. F., Smirnov, A., and Holben, B. N.: Multiangle Imaging SpectroRadiometer global aerosol product assessment by comparison with the Aerosol Robotic Network, J. Geophys. Res.-Atmos., 115, D23209, doi:10.1029/2010JD014601, 2010. 2256

King, M. D., Byrne, D. M., Herman, B. M., and Reagan, J. A.: Aerosol size distributions obtained by inversion of spectral optical depth measurements, J. Atmos. Sci., 21, 2153–2167, 1978. 2274

King, M., Kaufman, Y., Tanré, D., and Nakajima, T.: Remote sensing of Tropospheric aerosols from Space: Past, Present, and Future, B. Am. Meteorol. Soc., 80, 2229–2259, 1999. 2255

Kinne, S., Lohmann, U., Feichter, J., Schulz, M., Timmreck, C., Ghan, S., Easter, R., Chin, M., Ginoux, P., Takemura, T., Tegen, I., Koch, D., Herzog, M., Penner, J., Pitari, G., Holben, B., Eck, T., Smirnov, A., Dubovik, O., Slutsker, I., Tanré, D., Torres, O., Mishchenko, M., Geogdzhayev, I., Chu, D. A., and Kaufman, Y. J.: Monthly averages of aerosol properties: A global comparison among models, satellite data and AERONET ground data, J. Geophys. Res., 108, 4634, doi:10.1029/2001JD001253, 2003. 2256

Kinne, S., Schulz, M., Textor, C., Guibert, S., Balkanski, Y., Bauer, S. E., Berntsen, T., Berglen, T. F., Boucher, O., Chin, M., Collins, W., Dentener, F., Diehl, T., Easter, R., Feichter, J., Fillmore, D., Ghan, S., Ginoux, P., Gong, S., Grini, A., Hendricks, J., Herzog, M., Horowitz, L., Isaksen, I., Iversen, T., Kirkevåg, A., Kloster, S., Koch, D., Kristjansson, J. E., Krol, M., Lauer, A., Lamarque, J. F., Lesins, G., Liu, X., Lohmann, U., Montanaro, V., Myhre, G., Penner, J., Pitari, G., Reddy, S., Seland, O., Stier, P., Takemura, T., and Tie, X.: An AeroCom initial assessment – optical properties in aerosol component modules of global models, Atmos. Chem. Phys., 6, 1815–1834, doi:10.5194/acp-6-1815-2006, 2006. 2256

Klett, D.: Stable analytical inversion solution for processing lidar returns, Appl. Opt., 20, 211–220, 1981. 2257

Klett, D.: Lidar inversion with variable backscatter/extinction ratios, Appl. Opt., 31, 1638–1643, 1985. 2257

Koch, D., Schulz, M., Kinne, S., McNaughton, C., Spackman, J. R., Balkanski, Y., Bauer, S., Berntsen, T., Bond, T. C., Boucher, O., Chin, M., Clarke, A., De Luca, N., Dentener, F., Diehl, T., Dubovik, O., Easter, R., Fahey, D. W., Feichter, J., Fillmore, D., Freitag, S., Ghan, S., Ginoux, P., Gong, S., Horowitz, L., Iversen, T., Kirkevåg, A., Klimont, Z., Kondo, Y., Krol, M., Liu, X., Miller, R., Montanaro, V., Moteki, N., Myhre, G., Penner, J. E., Perlwitz, J., Pitari, G., Reddy, S., Sahu, L., Sakamoto, H., Schuster, G., Schwarz, J. P., Seland, Ø., Stier, P.,

AMTD
6, 2253–2325, 2013

Takegawa, N., Takemura, T., Textor, C., van Aardenne, J. A., and Zhao, Y.: Evaluation of black carbon estimations in global aerosol models, Atmos. Chem. Phys., 9, 9001–9026, doi:10.5194/acp-9-9001-2009, 2009. 2256

Kokhanovsky, A., Bréon, F. M., Cacciari, A., Carboni, E., Diner, D., Di Nicolantonio, W., Grainger, R. G., Grey, W. M. F., Höller, R., Lee, K.-H., Li, Z., North, P. R. J., Sayer, A. M., Thomas, G. E., and von Hoyningen-Huene, W.: Aerosol remote sensing over land: A comparison of satellite retrievals using different algorithms and instruments, Atmos. Res., 85, 372–394, 2007. 2255

Kotelnikov, V. A.: On the carrying capacity of the ether and wire in telecommunications, in: Material for the First All-Union Conference on Questions of Communication, Izd. Red. Upr. Svyazi RKKA, Moscow, 1933. 2269

Kovalev, V. A.: Sensitivity of the lidar solution to errors of the aerosol backscatter-to-extinction ratio: Influence of a monotonic change in the aerosol extinction coefficient, Appl. Opt., 34, 3457–3462, 1995. 2257

Kovalev, V. A. and Oller, H. M.: Distortion of particulate extinction profiles measured with lidar in a two-component atmosphere, Appl. Opt., 33, 6499–6570, 1994. 2269

Li, Z., Goloub, P., Dubovik, O., Blarel, L., Zhang, W., Podvin, T., Sinyuk, A., Sorokin, M., Chen, H., Holben, B. N., Tanré, D., Canini, M., and Buis, J.-P.: Improvements for ground-based remote sensing of atmospheric aerosol properties by additional polarimetric measurements, J. Quant. Spectrosc. Ra., 110, 1954–1961, 2009. 2260

Liu, Z., Sugimoto, N., and Murayama, T.: Extinction-to- backscatter ratio of Asian dust observed with high-spectral- resolution lidar and Raman lidar, Appl. Opt., 41, 2760–2767, 2002. 2258

Marenco, F., Santacesaria, V., Bais, A. F., Balis, D., di Sarra, A., Papayannis, A., and Zerefos, C.: Optical properties of tropospheric aerosols determined by lidar and spectrophotometric measurements (Photochemical Activity and Solar Ultraviolet Radiation Campaign), Appl. Opt., 36, 6875–6886, 1997. 2258

Matsumoto, M. and Takeuchi, N.: Effects of misestimated far-end boundary values on two common lidar inversion solutions, Appl. Opt., 33, 6451–6456, 1994. 2269

McCormick, M. P., Wang, P.-H., and Poole, L. R.: Stratospheric aerosols and clouds, in Aerosol-Cloud-Climate Interactions, 205–222, Academic Press, San Diego, Calif, 1993. 2256

McKendry, I., Strawbridge, K. B., O'Neill, N. T., Macdonald, A. M., Liu, P. S. K., Leaitch, W. R., Anlauf, K. G., Jaegle, L., Fairlie, T. D., and Westphal, D. L.: Trans-Pacific transport of Saharan dust to western North America: A case study, J. Geophys. Res., 112, D01103, doi:10.1029/2006JD007129, 2007. 2256

AMTD
6, 2253–2325, 2013

Mishchenko, M. I., Hovenier, J. W., and Travis, L. D.: Light scattering by nonspherical particles, Elsevier, New York, 2000. 2279

Mishchenko, M. I., Cairns, B., Ha, Travis, L. D., Burg, R., Ka, Martins, J. V., and Shettle, E. P.: Monitoring of aerosol forcing of climate from space: Analysis of measurement requirements, J. Quant. Spectrosc. Radiat. Transfer, 79/80, 149–161, 2004. 2279

Mishchenko, M. I., Cairns, B., Kopp, G., Schueler, C. F., Fafaul, B. A., Hansen, J. E., Hooker, R. J., Itchkawich, T., Maring, H. B., and Travis, L. D.: Accurate monitoring of terrestrial aerosol and total solar irradiance: introducing the Glory, Mission, B. Am. Meteorol. Soc., 88, 677–691, 2007. 2265

Müller, D., Wandinger, U., and Ansmann, A.: Microphysical particle parameters from extinction and backscatter lidar data by inversion with regularization: Theory, Appl. Opt., 38, 2346–2357, 1999. 2258

Müller, D., Mattis, I., Wandinger, U., Ansmann, A., Althausen, D., Dubovik, O., Eckhardt, S., and Stohl, A.: Saharan dust over a Central European EARLINET-AERONET site: Combined observations with Raman lidar and Sun photometer, J. Geophys. Res., 108, 4345, doi:10.1029/2002JD002918, 2003. 2256

Müller, D., Mattis, I., Ansmann, A., Wehner, B., Althausen, D., Wandinger, U., and Dubovik, O.: Closure study on optical and microphysical properties of a mixed urban and Arctic haze air mass observed with Raman lidar and Sun photometer, J. Geophys. Res., 109, D13206, doi:10.1029/2003JD004200, 2004. 2256

Müller, D., Mattis, I., Wandinger, U., Ansmann, A., Althausen, D., and Stohl, A.: Raman lidar observations of aged Siberian and Canadian forest fire smoke in the free troposphere over Germany in 2003: Microphysical particle characterization, J. Geophys. Res., 110, D17201, doi:10.1029/2004JD005756, 2005. 2258

Murayama, T., Sugimoto, N., Matsui, I., Liu, Z., Sakai, T., Shibata, T., Iwasaka, Y., Won, J.-G., Yoon, S.-C., Li, T., Zhou, J., and Hu, H.: Lidar Network Observation of Asian Dust, in: Advances in Laser Remote sensing, Selected papers 20th Int. Laser Radar Conference (ILRC), Vichy, France, 10–14 July 2000, edited by: Dabas, A., Loth, C., and Pelon, J., 169–177, Vichy, France, 2001. 2256

Nakajima, T., Tanaka, M., and Yamauchi, T.: Retrieval of the optical properties of aerosols from aureole and extinction data, Appl. Opt., 22, 2951–2959, 1983. 2274

AMTD
6, 2253–2325, 2013

Nakajima, T., Tonna, G., Rao, R., Kaufman, Y. J., and Holben, B. N.: Use of sky brightness measurements from ground for remote sensing of particulate polydispersions, Appl. Opt., 35, 2672–2686, 1996. 2255, 2274

Nakajima, T., Yoon, S. C., Ramanathan, V., Shi, G.-Y., Takemura, T., Higurashi, A., Takamura, T., Aoki, K., Sohn, B.-J., Kim, S.-W., Tsuruta, H., Sugimoto, N., Shimizu, A., Tanimoto, H., Sawa, Y., Lin, N.-H., Lee, C.-T., Goto, D., and Schutgens, N.: Overview of the Atmospheric Brown Cloud East Asian Regional Experiment 2005 and a study of the aerosol direct radiative forcing in east Asia, J. Geophys. Res., 112, D24S91, doi:10.1029/2007JD009009, 2007. 2256

Nyquist, H.: Certain topics in telegraph transmission theory, Trans. AIEE, 47, 617–644, 1928. 2269

Omar, A. H., Won, J. G., Winker, D. M., Yoon, S. C., Dubovik, O., and McCormick, M. P.: Development of global aerosol models using cluster analysis of AERONET measurements, J. Geophys. Res., 110, D10S14, doi:10.1029/2004JD004874, 2005. 2257

Oshchepkov, S., Sasano, Y., and Yokota, T.: New method for simultaneous gas and aerosol retrievals from space limb-scanning spectral observation of the atmosphere, Appl. Opt., 41, 4234–4244, 2002. 2273

Pahlow, M., Kovalev, V. A., and Parlange, M. B.: Calibration method for multiangle lidar measurements, Appl. Opt., 43, 2948–2956, 2004. 2257

Papayannis, A., Balis, D., Amiridis, V., Chourdakis, G., Tsaknakis, G., Zerefos, C., Castanho, A. D. A., Nickovic, S., Kazadzis, S., and Grabowski, J.: Measurements of Saharan dust aerosols over the Eastern Mediterranean using elastic backscatter-Raman lidar, spectrophotometric and satellite observations in the frame of the EARLINET project, Atmos. Chem. Phys., 5, 2065–2079, doi:10.5194/acp-5-2065-2005, 2005. 2256

Pickering, K. E., Thompson, A. M., Kim, H., DeCaria, A. J., Pfister, L., Kucsera, T. L., Witte, J. C., Avery, M. A., Blake, D. R., Crawford, J. H., Heikes, B. G., Sachse, G. W., Sandholm, S. T., and Talbot, R. W.: Trace gas transport and scavenging in PEM-Tropics B South Pacific Convergence Zone convection, J. Geophys. Res., 106, 32591–32602, 2001. 2282

Pilinis, C., Pandis, S. N., and Seinfeld, J. H.: Sensitivity of direct climate forcing by atmospheric aerosols to aerosol size and composition, J. Geophys. Res., 100, 18739–18754, 1995. 2255, 2256

Ramanathan, V., Crutzen, P. J., Lelieveld, J., Mitra, A. P., Althausen, D., Anderson, J., Andreae, M. O., Cantrell, W., Cass, G. R., Chung, C. E., Clarke, A. D., Coakley, J. A., Collins,

AMTD
6, 2253–2325, 2013

W. D., Conant, W. C., Dulac, F., Heintzenberg, J., Heymsfield, A. J., Holben, B., Howell, S., Hudson, J., Jayaraman, A., Kiehl, J. T., Krishnamurti, T. N., Lubin, D., McFarquhar, G., Novakov, T., Ogren, J. A., Podgorny, I. A., Prather, K., Priestley, K., Prospero, J. M., Quinn, P. K., Rajeev, K., Rasch, P., Rupert, S., Sadourny, R., Satheesh, S. K., Shaw, G. E., Sheridan, P., and Valero, F. P. J.: Indian Ocean Experiment: An integrated analysis of the climate forcing and effects of the great Indo-Asian haze, J. Geophys. Res., 106, 28371–28398, doi:10.1029/2001JD900133, 2001. 2255, 2256

Remer, L. A., Tanre, D., Kaufman, Y. J., Ichoku, C., Mattoo, S., Levy, R., Chu, D. A., Holben, B., Dubovik, O., Smirnov, A., Martins, J. V., Li, R. R., and Ahmad, Z.: Validation of MODIS aerosol retrieval over ocean, Geophys. Res. Lett., 29, 1618, doi:10.1029/2001GL013204, 2002. 2256

Remer, L. A., Kaufman, Y. J., Tanre, D., Mattoo, S., Chu, D. A., Martins, J. V., Li, R. R., Ichoku, C., Levy, R. C., Kleidman, R. G., Eck, T. F., Vermote, E., and Holben, B. N.: The MODIS aerosol algorithm, products, and validation, J. Atmos. Sci., 62, 947–973, doi:10.1175/JAS3385.1, 2005. 2256

Rodgers, C. D.: Retrieval of atmospheric temperature from remote measurements of thermal radiation, Rev. Geophys., 14, 609–624, 1976. 2274

Sasano, Y., Browell, E. V., and Ismail, S.: Error caused by using a constant extinction backscattering ratio in the lidar solution, Appl. Opt., 24, 3929–3932, 1985. 2257

Schoeberl, M. R. and Newman, P. A.: A multiple-level trajectory analysis of vortex filaments, J. Geophys. Res., 100, 25801–25816, 1995. 2282

Schuster, G. L., Vaughan, M., MacDonnell, D., Su, W., Winker, D., Dubovik, O., Lapyonok, T., and Trepte, C.: Comparison of CALIPSO aerosol optical depth retrievals to AERONET measurements, and a climatology for the lidar ratio of dust, Atmos. Chem. Phys., 12, 7431–7452, doi:10.5194/acp-12-7431-2012, 2012. 2256

Shipley, S. T., Tracy, D. H., Eloranta, E. W., Trauger, J. T., Sroga, J. T., Roesler, F. L., and Weinman, J. A.: High spectral resolution lidar to measure optical scattering properties of atmospheric aerosols, Appl. Opt., 23, 3716–3724, 1983. 2258

Sicard, M., Chazette, P., Pelon, J., Gwang-Won, J., and Yoon, S.-C.: Variational method for the retrieval of the optical thickness and the backscatter coefficient from multiangle lidar profiles, Appl. Opt., 41, 493–502, 2002. 2257

Sinyuk, A., Dubovik, O., Holben, B., Eck, T. F., Bréon, F.-M., Martonchik, J., Kahn, R., Diner, D. J., Vermote, E. F., Roger, J.-C., Lapyonok, T., and Slutsker, I.: Simultaneous retrieval of

AMTD
6, 2253–2325, 2013

aerosol and surface properties from a combination of AERONET and satellite data, Remote Sens. Environ., 107, 90–108, doi:10.1016/j.rse.2006.07.022, 2007. 2260, 2261, 2262, 2270

Takamura, T., Sasano, Y., and Hayasaka, T.: Tropospheric aerosol optical properties derived from lidar, sun photometer, and optical particle counter measurements, Appl. Opt., 33, 7132–7140, 1994. 2256

Textor, C., Schulz, M., Guibert, S., Kinne, S., Balkanski, Y., Bauer, S., Berntsen, T., Berglen, T., Boucher, O., Chin, M., Dentener, F., Diehl, T., Easter, R., Feichter, H., Fillmore, D., Ghan, S., Ginoux, P., Gong, S., Grini, A., Hendricks, J., Horowitz, L., Huang, P., Isaksen, I., Iversen, I., Kloster, S., Koch, D., Kirkevåg, A., Kristjansson, J. E., Krol, M., Lauer, A., Lamarque, J. F., Liu, X., Montanaro, V., Myhre, G., Penner, J., Pitari, G., Reddy, S., Seland, Ø., Stier, P., Takemura, T., and Tie, X.: Analysis and quantification of the diversities of aerosol life cycles within AeroCom, Atmos. Chem. Phys., 6, 1777–1813, doi:10.5194/acp-6-1777-2006, 2006. 2256

Turner, D. D., Ferrare, R. A., Heilman-Brasseur, L. A., Feltz, W. F., and Tooman, T. P.: Automated retrievals of water vapor and aerosol profiles from an operational Raman lidar, J. Atmos. Ocean. Technol., 19, 37–50, 2002. 2257

Twomey, S.: On the numerical solution of Fredholm integral equations of the first kind by the inversion of the linear system produced by quadrature, J. Assoc. Comp. Mach., 10, 97–101, 1963. 2274

Veselovskii, I., Kolgotin, A., Griaznov, V., Müller, D., Franke, K., and Whiteman, D. N.: Inversion of multiwavelength Raman lidar data for retrieval of bimodal aerosol size distribution, Appl. Opt., 43, 1180–1195, 2004. 2258

Veselovskii, I., Dubovik, O., Kolgotin, A., Lapyonok, T., Di Girolamo, P., Summa, D., Whiteman, D. N., Mishchenko, M., and Tanré, D.: Application of randomly oriented spheroids for retrieval of dust particle parameters from multi- wavelength lidar measurements, J. Geophys. Res., 115, D21203, doi:10.1029/2010JD014139, 2010. 2265

Volten, H., Munoz, O., Rol, E., de Haan, J. F., Vassen, W., Hovenier, J. W., Muinonen, K., and Nousiainen, T.: Scattering matrices of mineral aerosol particles at 441.6 nm and 632.8 nm, J. Geophys. Res., 106, 17375–17401, 2001. 2265

Waquet, F., Léon, J.-F., Goloub, P., Pelon, J., Tanré, D., and Deuzé, J.-L.: Maritime and dust aerosol retrieval from polarized and multispectral active and passive sensors, J. Geophys. Res., 110, D10S10, doi:10.1029/2004JD004839, 2005. 2256, 2258

AMTD
6, 2253–2325, 2013

Welton, E. J., Campbell, J. R., Berkoff, T. A., Spinhirne, J. D., Tsay, S.-C., Holben, B., and Shiobara, M.: The Micro-pulse Lidar Network (MPL-Net), in: Lidar Remote Sensing in Atmospheric and Earth Sciences, Reviewed and revised papers at the twenty-first International Laser Radar Conference (ILRC21), Quebec, Canada, 8–12 July, edited by: Bisonnette, L. R., Roy, G., and Vallee, G., 285–288, Defence R&D Canada – Vacartier, 2002. 2256

Winker, D. M., Hunt, W. H., and McGill, M. J.: Initial performance assessment of CALIOP, Geophys. Res. Lett., 34, L19803, doi:10.1029/2007GL030135, 2007. 2255

Yoon, J., von Hoyningen-Huene, W., Vountas, M., and Burrows, J. P.: Analysis of linear long-term trend of aerosol optical thickness derived from SeaWiFS using BAER over Europe and South China, Atmos. Chem. Phys., 11, 12149–12167, doi:10.5194/acp-11-12149-2011, 2011. 2256

AMTD
6, 2253–2325, 2013

Table 1. Parameters retrieved by the algorithm.

Aerosol characteristics	
$\frac{dV^k(r_i)}{d\ln r}$	$(i = 1,...,N_i^k; k = 1,2)$ values of volume size distribution in size bins of k-th aerosol component
$c^k(h_i)$	$(k = 1,2)$ vertical distribution of aerosol concentration of k-th aerosol component, normalized to 1
C_{sph}	Faction of spherical particles of coarse aerosol component
$n^k(\lambda_i)$	$(i = 1,...,N_\lambda = 7; k = 1,2)$ the real part of the refractive index for k-th aerosol component at every λ_i of combined lidar-photometric measurement
$k^k(\lambda_i)$	$(i = 1,...,N_\lambda = 7; k = 1,2)$ the imaginary part of the refractive index for k-th aerosol component at every λ_i of combined lidar-photometric measurement
Lidar calibration parameters	
$A(\lambda_i)$	$(i = 1,...,3)$ lidar calibration coefficient at each λ_i of the lidar measurement

AMTD
6, 2253–2325, 2013

Table 2. Parameters of log-normal distributions used for aerosol size distribution modelling.

Aerosol mode	r_{min}, µm	r_{max}, µm	r_{mean}, µm	r_{std}	$\tau, (\tau_{total} = 1)$	$\tau, (\tau_{total} = 0.05)$
Fine	0.05	0.576	0.148	0.4	0.8, 0.5, 0.2	0.04, 0.025, 0.01
Coarse	0.355	15.0	2.32	0.6	0.2, 0.5, 0.8	0.01, 0.025, 0.04

AMTD
6, 2253–2325, 2013

Table 3. Relative errors of spherical particles faction retrieval.

$\frac{\tau_c}{\tau_f}$	AERONET +lidar no noise	AERONET noise added	AERONET +lidar noise added
0.25	0.99	1.00	0.98
1	0.28	0.99	0.99
4	0.02	0.89	0.03

AMTD
6, 2253–2325, 2013

Table 4. Parameters of noise estimations for the lidar system.

Parameter	v	g	q	u	α_1	α_2
Value	10^{-5}	10^{-4}	10^{-1}	1	10^{-1}	10^{-3}

AMTD
6, 2253–2325, 2013

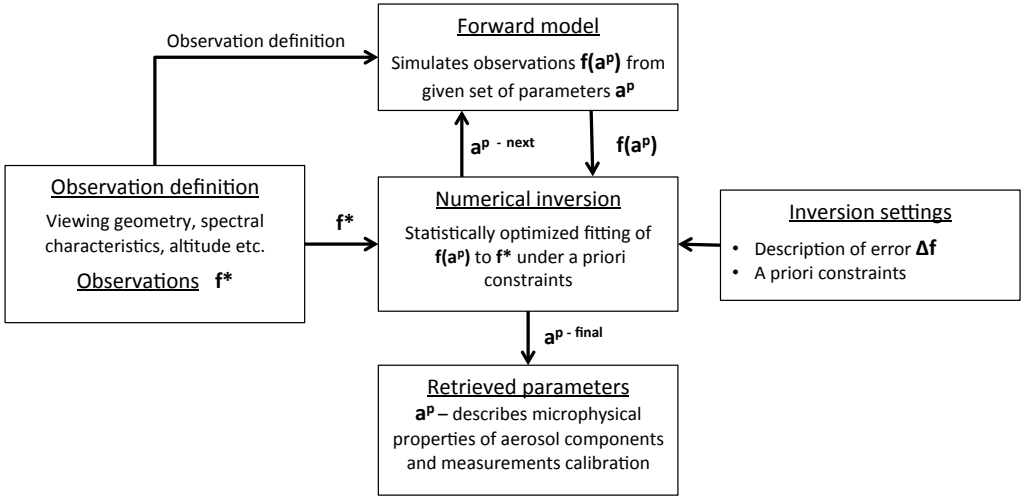

Fig. 1. General structure of the inversion algorithm.

AMTD
6, 2253–2325, 2013

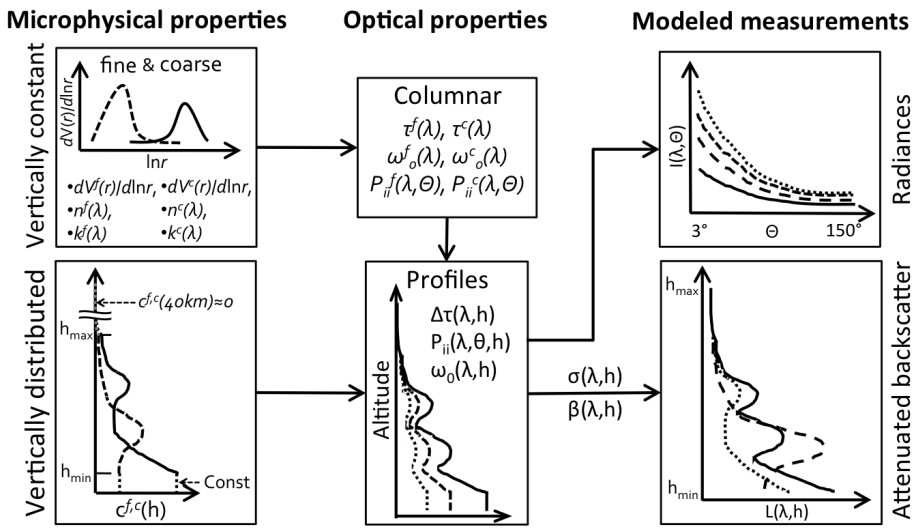

Fig. 2. General scheme of the measurements modelling using two-component vertically distributed aerosol model.

AMTD
6, 2253–2325, 2013

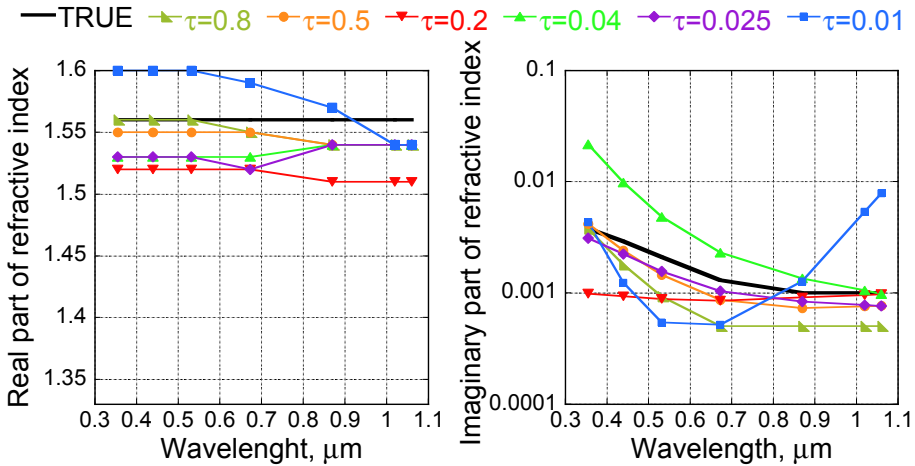

Fig. 3. Retrievals of complex refractive index of "Dust" aerosol model under different AOT.

AMTD
6, 2253–2325, 2013

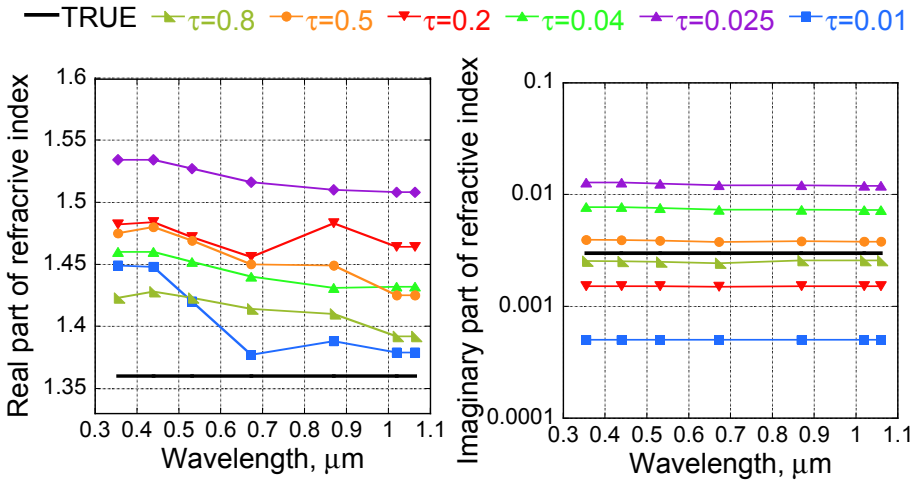

Fig. 4. Retrievals of complex refractive index of "Urban" aerosol model under different AOT.

AMTD
6, 2253–2325, 2013

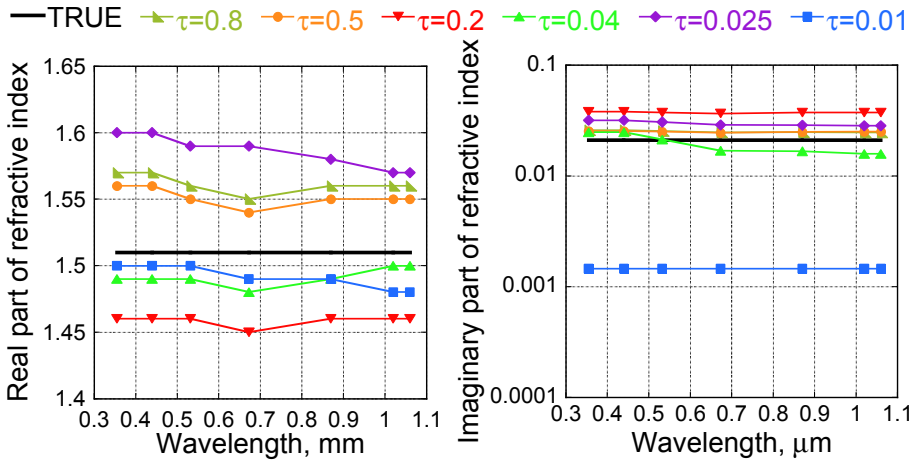

Fig. 5. Retrievals of complex refractive index of "Smoke" aerosol model under different AOT.

AMTD
6, 2253–2325, 2013

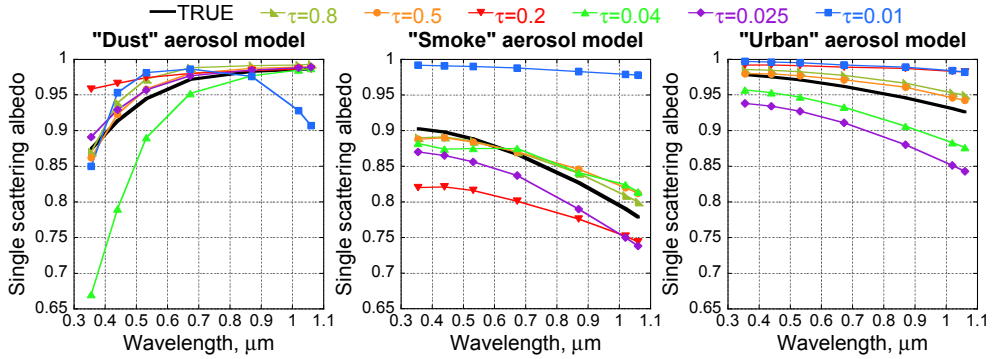

Fig. 6. Retrievals of the single scattering albedo of aerosol components under different AOT.

AMTD
6, 2253–2325, 2013

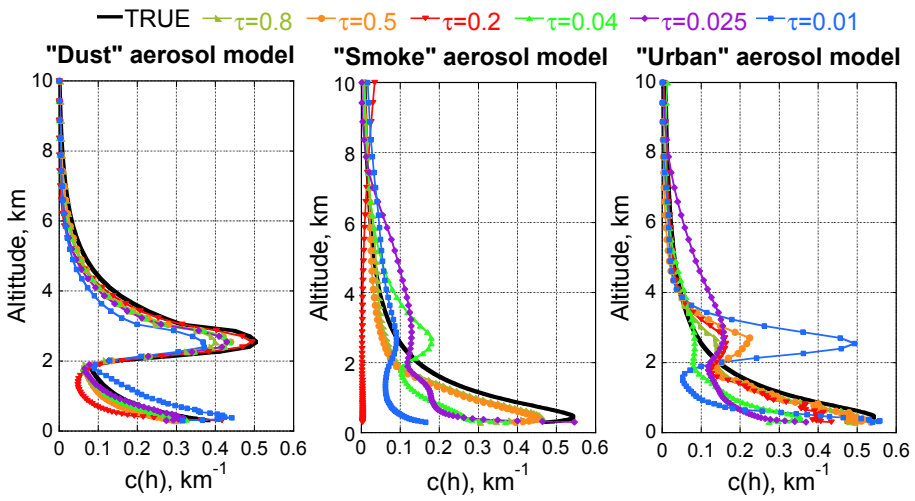

Fig. 7. Retrievals of the vertical distributions of aerosol components under different AOT.

AMTD
6, 2253–2325, 2013

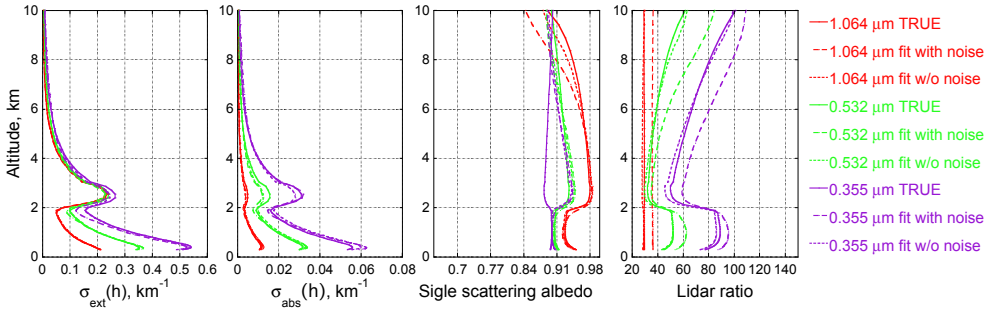

Fig. 8. Retrievals of the vertical distributions of aerosol optical properties under different noise conditions.

AMTD
6, 2253–2325, 2013

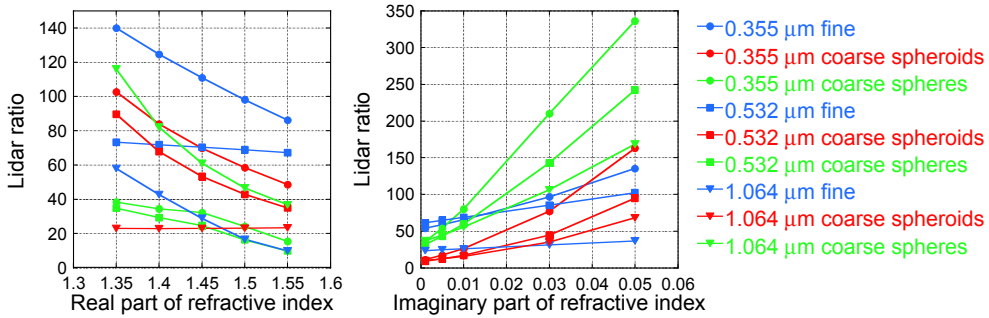

Fig. 9. Dependences of lidar ratio of fine and coarse modes on complex refractive index and particle shape.

AMTD
6, 2253–2325, 2013

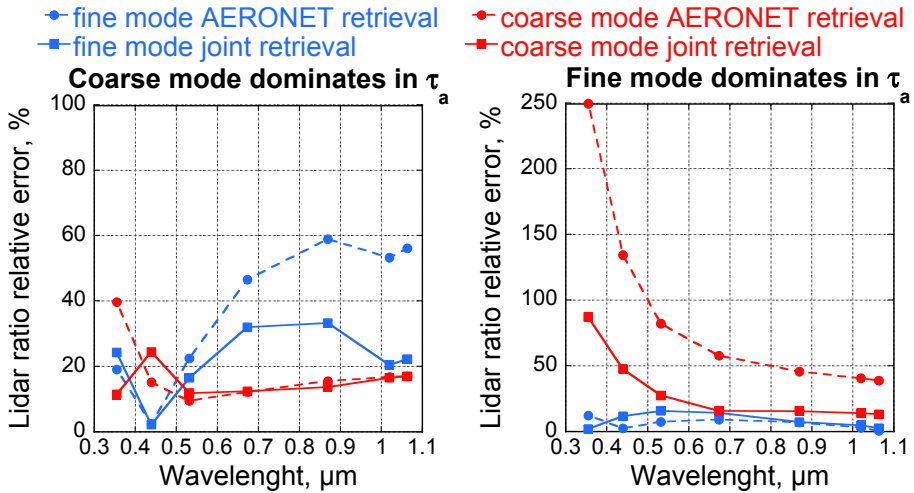

Fig. 10. Retrieval errors of lidar ratio with and without accountancy for lidar data.

AMTD
6, 2253–2325, 2013

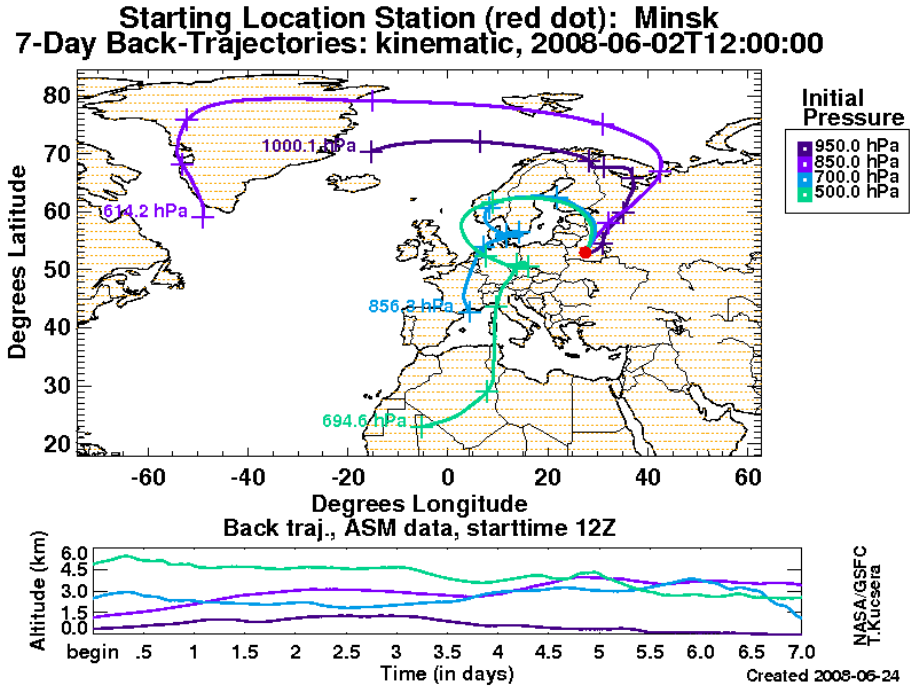

Fig. 11. Air mass back trajectories for the Minsk measurement site on 02 June 2008.

AMTD
6, 2253–2325, 2013

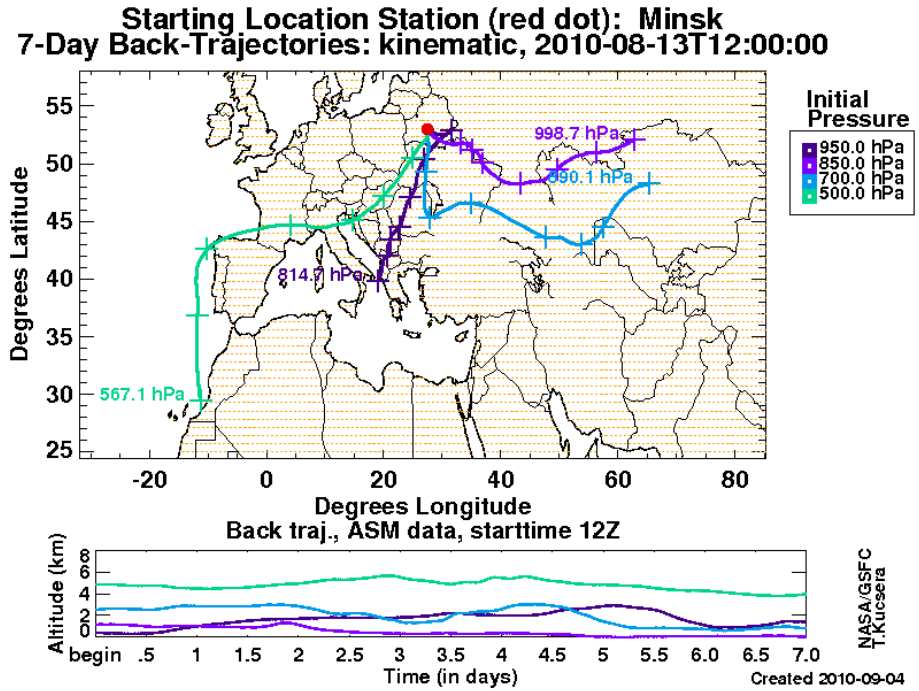

Fig. 12. Air mass back trajectories for the Minsk measurement site on 13 August 2010.

AMTD
6, 2253–2325, 2013

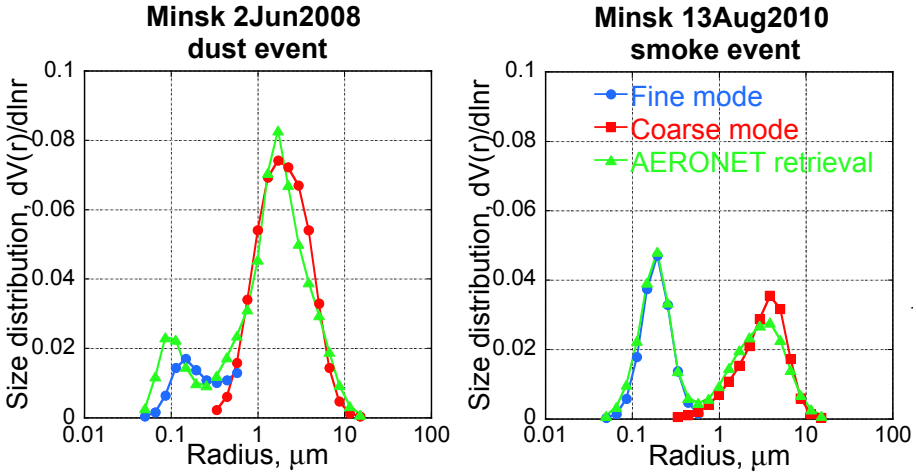

Fig. 13. Retrieved aerosol size distributions.

AMTD
6, 2253–2325, 2013

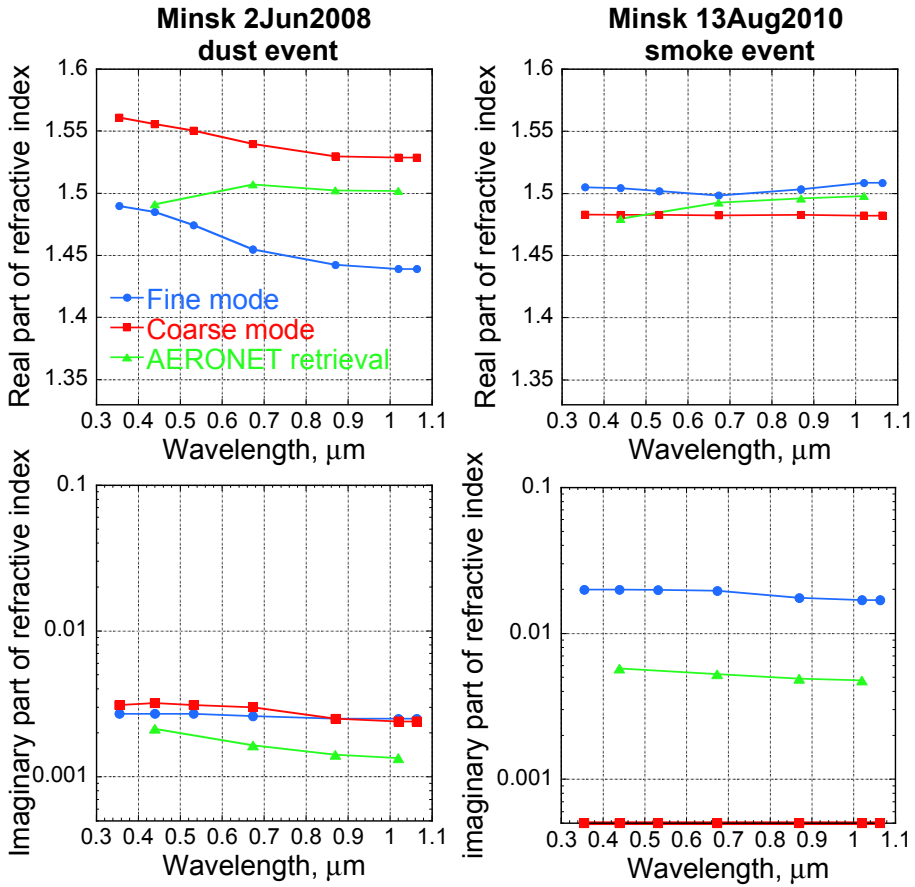

Fig. 14. Retrieved aerosol complex refractive indices.

AMTD
6, 2253–2325, 2013

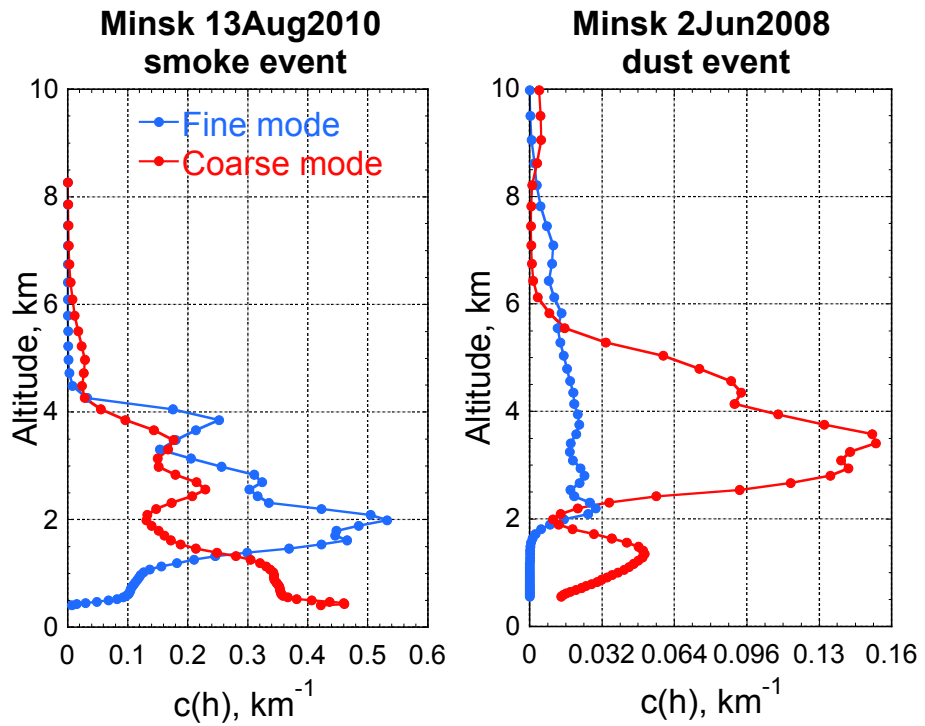

Fig. 15. Retrieved vertical concentration profiles.

AMTD
6, 2253–2325, 2013

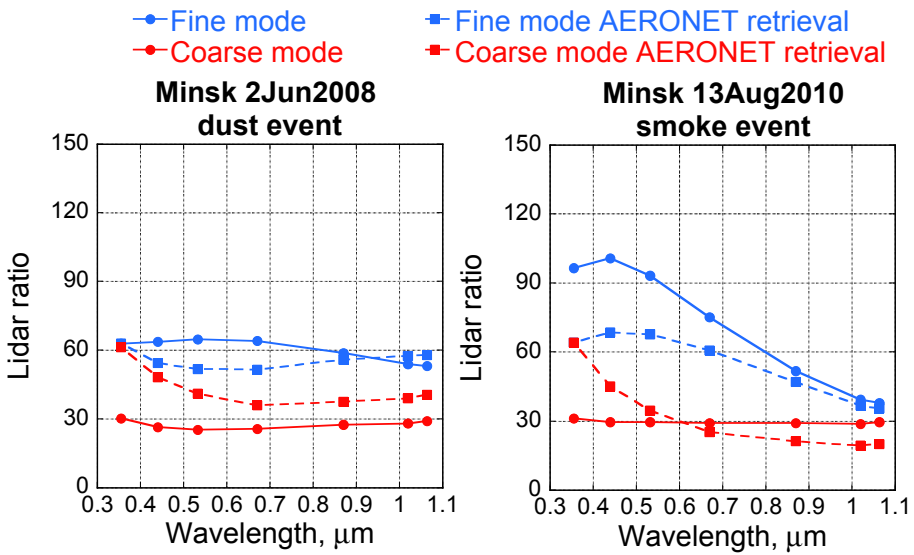

Fig. 16. Retrieved aerosol lidar ratios.

AMTD
6, 2253–2325, 2013

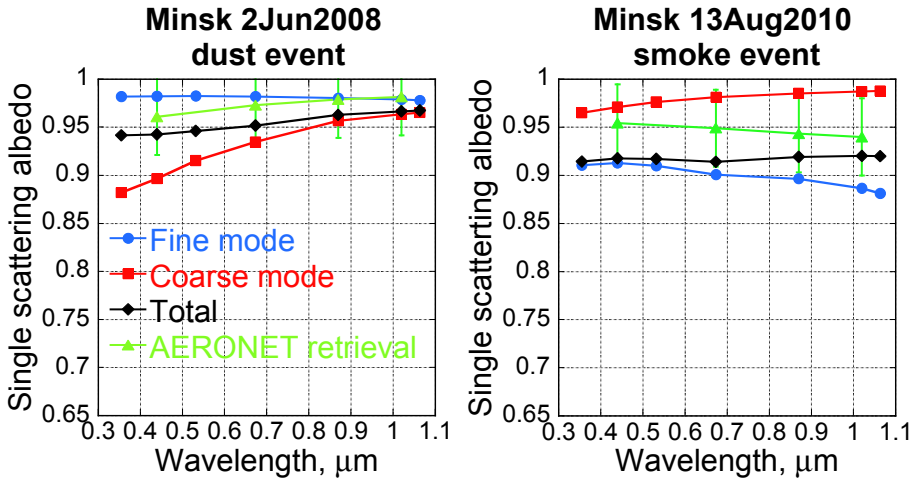

Fig. 17. Retrieved aerosol single scattering albedo.

AMTD
6, 2253–2325, 2013

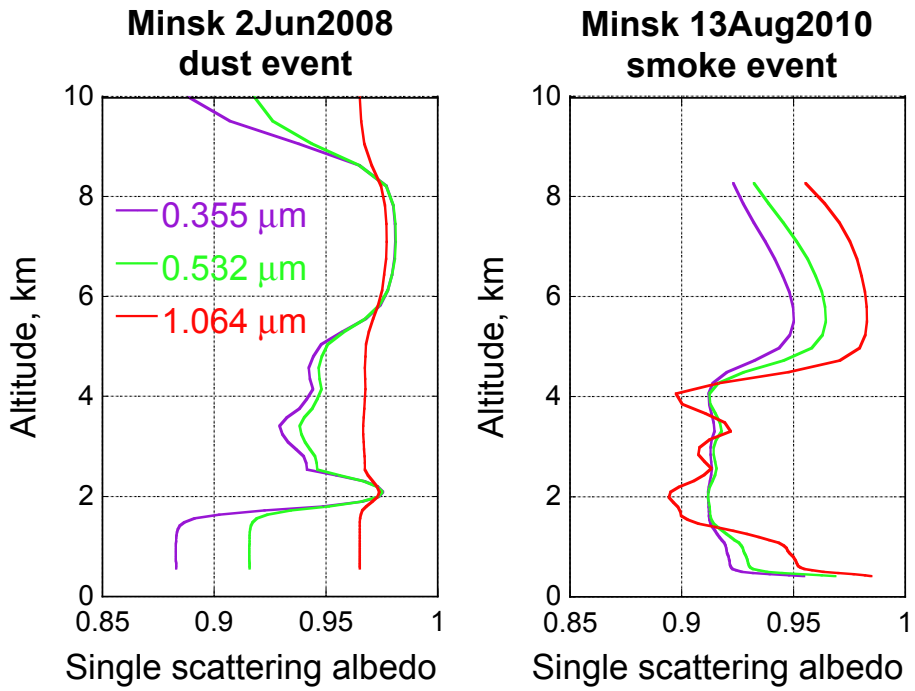

Fig. 18. Retrieved vertical profiles of aerosol single scattering albedo.

AMTD
6, 2253–2325, 2013

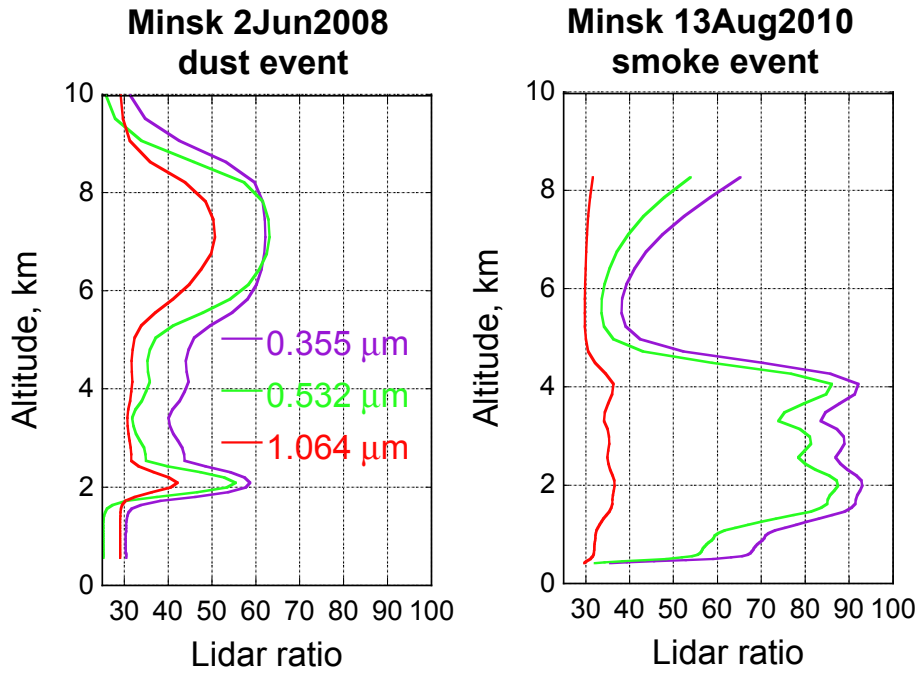

Fig. 19. Retrieved vertical profiles of aerosol lidar ratio.

AMTD
6, 2253–2325, 2013

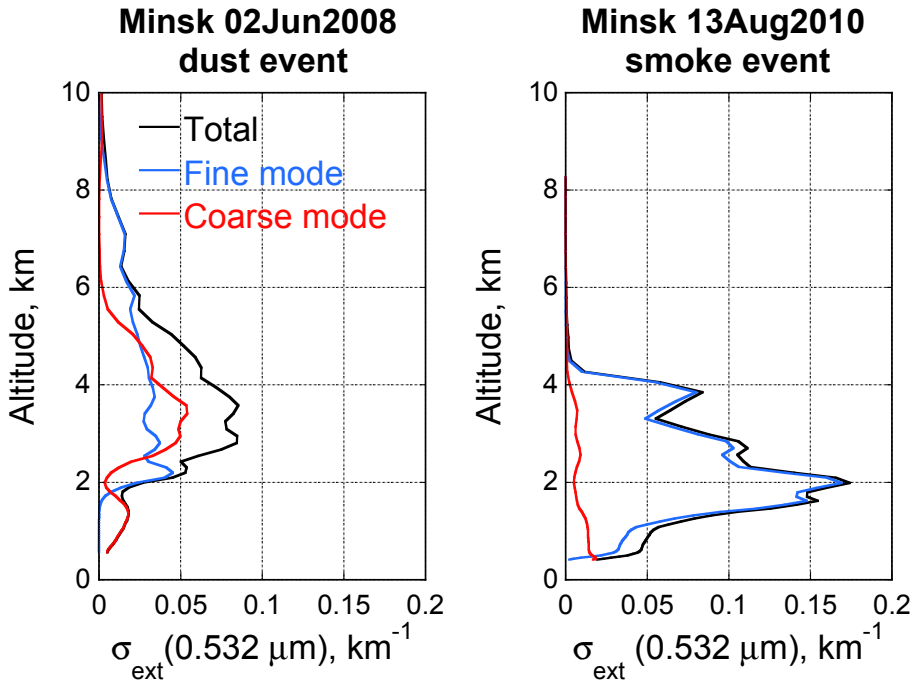

Fig. 20. Retrieved vertical profiles of aerosol extinction.

AMTD
6, 2253–2325, 2013

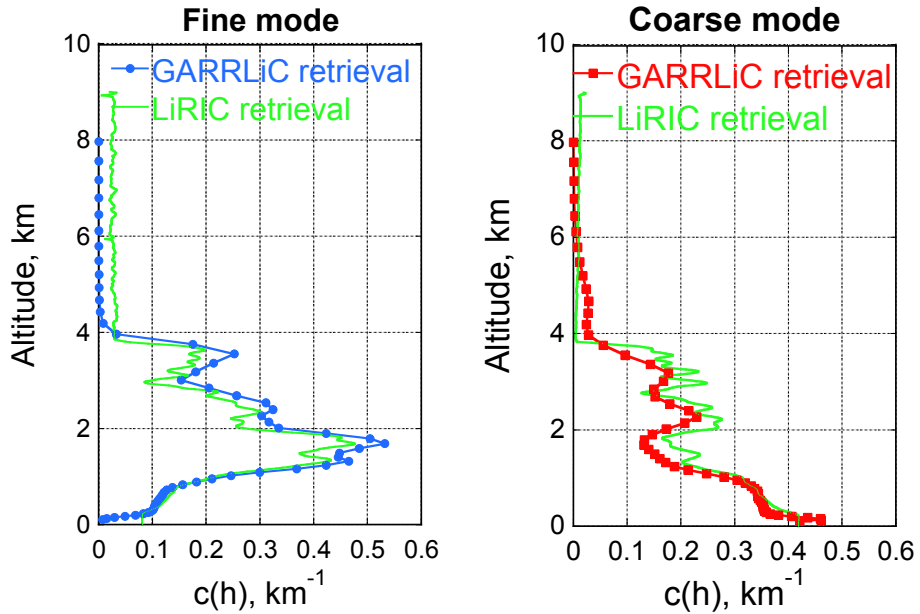

Fig. 21. Comparison of the retrieved vertical profiles with LiRIC inversion for observations on 13 August 2010.

AMTD
6, 2253–2325, 2013

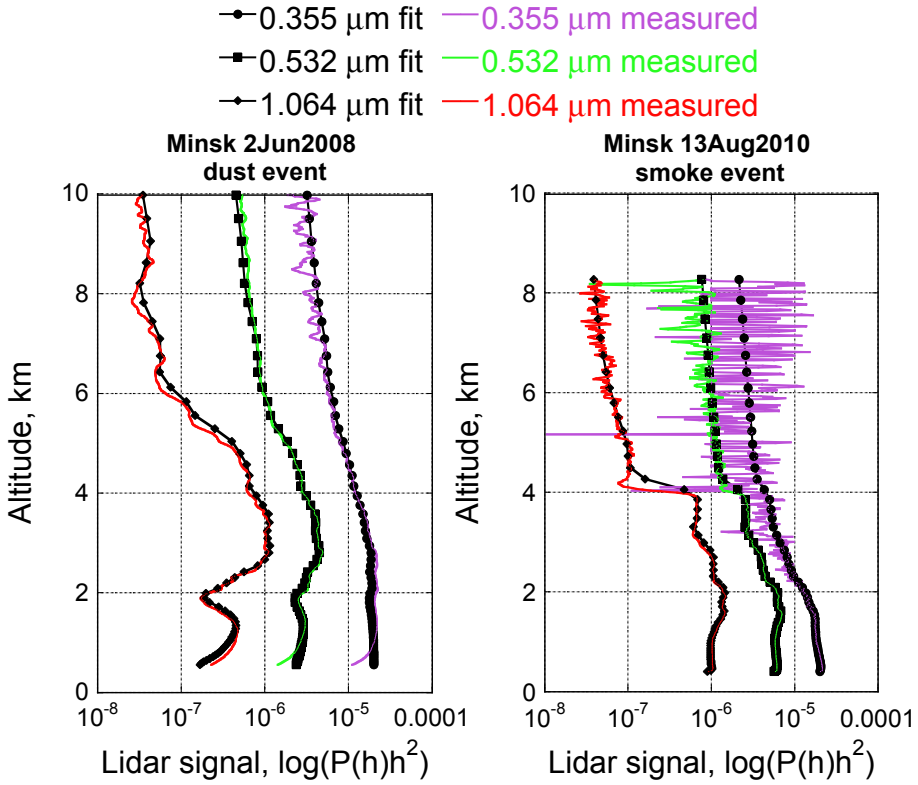

Fig. 22. Achieved lidar measurement fits.

AMTD
6, 2253–2325, 2013